4428 J. Med. Chem. 2010, 53, 4428–4440
DOI: 10.1021/jm1002167

Journal of Medicinal Chemistry Article

Biochemical and Structural Analysis of the Binding Determinants of a Vascular Endothelial Growth Factor Receptor Peptidic Antagonist

Benoit Gautier,[†] Victor Goncalves,[†] Donatella Diana,[‡] Rossella Di Stasi,[§] Florence Teillet,[∥] Christine Lenoir,[†] Florent Huguenot,[†,⊥] Christiane Garbay,[†] Roberto Fattorusso,[‡] Luca Domenico D'Andrea,[§] Michel Vidal,*[,†,⊥] and Nicolas Inguimbert*[,†,#]

[†] *Université Paris Descartes, UFR Biomédicale, Laboratoire de Pharmacochimie Moléculaire et Cellulaire, INSERM U648, 45 rue des Saints Pères, 75006 Paris, France,* [‡] *Dipartimento di Scienze Ambientali, Seconda Università di Napoli via Vivaldi 43, 81100 Caserta, Italy,* [§] *Istituto di Biostrutture e Bioimmagini, CNR, via Mezzocannone, 16, 80134 Napoli, Italy, and* [∥] *Université Paris Descartes, UFR Biomédicale, Laboratoire de Pharmacologie, Toxicologie et Signalisation Cellulaire, INSERM UMR-S 747, 45 rue des Saints Pères, 75006 Paris, France.* [⊥] *Current address: Université Paris Descartes, UFR des Sciences Pharmaceutiques et Biologiques, UMR CNRS 8638, 4 avenue de l'observatoire, 75270 Paris Cedex 06, France.* [#] *Current address: Université de Perpignan Via Domitia, laboratoire de chimie des biomolécules, 52 avenue Paul Alduy, 66860 Perpignan, France.*

Received February 18, 2010

Cyclic peptide antagonist c[YYDEGLEE]-NH_2, which disrupts the interaction between vascular endothelial growth factor (VEGF) and its receptors (VEGFRs), represents a promising tool in the fight against cancer and age-related macular degeneration. Furthermore, coupled to a cyclen derivative, this ligand could be used as a medicinal imaging agent. Nevertheless, before generating such molecular probes, some preliminary studies need to be undertaken in order to define the more suitable positions for introduction of the cyclen macrocycle. Through an Ala-scan study on this peptide, we identified its binding motif, and an NMR study highlights its binding sites on the VEGFR-1D2 Ig-like domain. Guided by the structural relationship results deduced from the effect of the peptides on endothelial cells, new peptides were synthesized and grafted on beads. Used in a pull-down assay, these new peptides trap the VEGFRs, thus confirming that the identified amino acid positions are suitable for further derivatization.

Introduction

The vascular endothelial growth factor (VEGF[a] or VEGF-A) and its tyrosine kinase receptors (VEGFR-1 and VEGFR-2) are validated targets in the fight against cancer.[1] Indeed, this system is a major player in tumor angiogenesis,[2,3] i.e., the formation of new blood vessels from a pre-existing vasculature. These newly formed capillaries allow the nutrition and oxygenation of the tumor and also the elimination of wasted products.[4] Since the hypothesis of J. Folkman,[5] antiangiogenic treatments constitute an approved therapeutic approach. One goal of antiangiogenic treatments is to normalize the capillary network within the tumor, which enhances the delivery of anticancer drug.[6] A way of achieving this goal is to act on the VEGF family or on their receptors.[7,8] Among the eight known human isoforms of VEGF, the predominant one is $VEGF_{165}$, which binds to VEGF receptor 1 (VEGFR-1) and VEGF receptor 2 (VEGFR-2) expressed at the surface of both endothelial and some tumor cells.[9,10] Several drugs targeting the VEGF/VEGFRs system are now used therapeutically.[11] They target either VEGF itself or its receptors. Bevacizumab, a humanized antibody directed against VEGF, is currently clinically used in the treatment of colon, kidney, breast, and non-small-cell lung cancers.[12,13] Aflibercept is a soluble VEGF receptor which acts as a VEGF trap and is currently under clinical evaluation.[14] Other treatments act on the receptors at the intracellular tyrosine kinase site and have led to the development of sunitinib and sorafenib exhibiting a multitarget spectrum.[15] These two inhibitors are largely used therapeutically, for example, in the treatment of metastatic kidney cancers.[16,17] Antibodies directed against the extracellular portion of the receptor are also being evaluated in clinical studies.[18] Among the compounds developed so far excluding the tyrosine kinase inhibitors, antibodies and soluble receptors act by blocking the interaction between the receptors and their

*To whom correspondence should be addressed. Pr. Nicolas Inguimbert, Laboratoire de Chimie des Biomolécules et de l'Environnement, Université Perpignan via Domitia, 52, avenue Paul Alduy, 66860 Perpignan, France. Tel.: +33.4.30.19.81.30. Fax: +33.130.19.81.38. E-Mail: nicolas.inguimbert@univ-perp.fr. Pr. Michel Vidal, Laboratoire de Pharmacochimie Moléculaire et Cellulaire, Université Paris Descartes, 45 rue des Saints Pères, 75006 Paris, France. Tel: +33.1.42.86.21.26. Fax: +33.1.42.86.40.82. E-mail: michel.vidal@parisdescartes.fr.

[a] Abbreviations: Abbreviation follow the rules edited by the IUPAC-IUB Commission on Biochemical Nomenclature (*J. Biol. Chem.* **1985**, *260*, 14−42). Additional abbreviations used are as follows: BSA, bovine serum albumin; btVEGF, biotinylated vascular endothelial growth factor; DCM, dichloromethane; DIPEA, *N*,*N*′-diisopropylethylamine; Dmab, 4-{*N*-[1-(4,4-dimethyl-2,6-dioxocyclohexylidene)-3-methylbutyl]amino}benzyl ester; DMF, dimethylformamide; DMSO, dimethylsulfoxide; DOTA, tetra-azacyclo-dodecanetetra-acetic acid; ECD, extracellular domain; EDTA, ethylenediaminetetraacetic acid; hEGF, human epidermal growth factor; ERK, extracellular signal-regulated kinase; FBS, fetal bovine serum; hFGF, human fibroblast growth factor; Fmoc, fluorenylmethyloxycarbonyl; HBTU, *O*-benzotriazole-*N*,*N*,*N*′,*N*′-tetramethyl-uronium-hexafluorophosphate; HOBt, *N*-hydroxybenzotriazole; HSQC, heteronuclear single quantum coherence; HUVEC, human umbilical vein endothelial cell; Ig, immunoglobulin; NMP, 1-methyl-2-pyrrolidinone; IGF-1, insulin-like growth factor 1; PBS, phosphate buffer saline; PlGF, placenta growth factor; MBHA, 4-(2′,4′-dimethoxyphenyl-Fmoc-aminomethyl)-phenoxyacetamido-methylbenzhydryl amine; SDS, sodium dodecyl sulfate; SH3, src homology 3; TBS, tris-HCl buffer saline; TBST, tris-HCl buffer saline Tween 20; TFA, trifluoroacetic acid; TIPS, triisopropylsilane; VEGF, vascular endothelial growth factor; VEGFR, vascular endothelial growth factor receptor; $VEGFR\text{-}1_{D2}$, vascular endothelial growth factor receptor 1 domain 2; $VEGFR\text{-}1_{D1\text{-}D3}$, vascular endothelial growth factor receptor 1 domain 1 to 3; $VEGFR\text{-}1_{ECD}$, vascular endothelial growth factor receptor 1 extracellular domain.

 Published on Web 05/12/2010

ligand VEGF. These compounds are prominent examples of inhibitors of protein/protein interactions which constitutes a challenge for the pharmaceutical industry of the 21st century.[19,20] Indeed, most cellular signals occur through protein/protein interactions, and agents interfering with these signaling pathways may regulate them.

Peptides antagonists acting on the receptor at the VEGF binding site thus appear as an alternative to currently developed antibodies as well as pharmacological tools for studying the regulation of cellular phenomena associated with tumor angiogenesis.[21] Therefore, we initiated a couple of years ago the development of VEGFRs antagonists,[22] by designing cyclic peptides through a rational approach.[23,24] This was achieved by relying on the crystallographic data available in the literature[25,26] and on mutagenesis studies performed on VEGF[27−29] and PlGF.[30] Those include in their sequence amino acids which were previously identified as hot spots of the VEGF for its interaction with the VEGFR-1.[31] In a previous paper, we described the synthesis of peptide c[YYDEGLEE]-NH_2 (peptide **1**), its preliminary biological data, as well as a brief structure−activity relationship study highlighting that Y1 and L6 of peptide **1** were necessary to conserve an optimal recognition of VEGFR-1.[23]

Nevertheless, this study was relatively limited and did not allow precise identification of the amino acids involved in the VEGFRs recognition. The selectivity of this peptide toward its cellular targets VEGFR-1 and -2 also remained unanswered. Moreover, grafted to cyclen derivatives such as DOTA, this peptide could be useful as a molecular probe for medicinal imaging purposes. This paper therefore focuses on an Ala-scan study for the identification of the amino acids involved in its interaction with the VEGFR-1 and -2, which is required for potential exploration of optimization attempts. All the peptides were evaluated for their selectivity and ability to interact with the VEGFRs by means of chemiluminescent competition assays[32,33] and Western blot experiments. NMR studies, using $^1H-^{15}N$ HSQC experiments with VEGFR-1 D2 Ig-like domain (VEGFR-1_{D2}) in presence of peptide **1** or an Ala-scan derived peptide **5**, also allowed identifying the amino acid residues of VEGFR-1 involved in peptides recognition. On the basis of the peptide **1** Ala-scan results, three amino acids were identified as nonessential for the binding to VEGFR-1_{D2}. Consequently, peptide **1** derivatives containing a lysine at these positions were grafted onto sepharose beads. These tools were then able to trap the VEGFRs in a pulldown assay.

Results

Peptide 1 Cyclic Form Required for Inhibitory Effect on $VEGF_{165}$ Binding to VEGFR-1. We previously reported that peptide **1** was able to inhibit $VEGF_{165}$ binding to VEGFR-1 in a chemiluminescent displacement assay relying on competition between tested compounds and biotinylated $VEGF_{165}$ ($btVEGF_{165}$) for binding to recombinant VEGFR-1_{ECD}.[32] To assess if the cyclic form plays a critical role for peptide **1** inhibitory properties, the corresponding linear form (peptide **2**) was synthesized and tested on the VEGFR-1_{ECD} assay. As expected, tested at 100 μM, peptide **2** showed no inhibition of $btVEGF_{165}$ binding, whereas peptide **1** showed 73% of inhibition (Table 1 A).

Inhibitory Effect of Peptide 1 on $VEGF_{165}$ Binding to VEGFR-1. To investigate whether the inhibitory effect of peptide **1** on $VEGF_{165}$ binding to VEGFR-1 was due to its ability to compete with the $VEGF_{165}$ binding sites located on the VEGFR-1 domains 1 to 3 (VEGFR-1_{D1-D3}), we conducted a competition assay based on the inhibition of $btVEGF_{165}$ binding to VEGFR-1_{D1-D3}.[33] Peptide **1** was able to inhibit, in a dose-dependent manner, the $btVEGF_{165}$ binding to both recombinant VEGFR-1_{ECD} and VEGFR-1_{D1-D3}, with respective IC_{50} of 32 and 23 μM. These results highlighted that peptide **1** inhibits $VEGF_{165}$ binding to VEGFR-1 by acting on $VEGF_{165}$ binding sites (Table 1. A).

Inhibitory Effect of Peptide 1 on $VEGF_{165}$-Induced VEGFR-1 and VEGFR-2 Phosphorylation. In a previous study,[23] we reported that peptide **1** exhibited an antagonistic effect on endothelial cells without information on its selectivity toward VEGFRs. Because $VEGF_{165}$ angiogenic properties pass through VEGFRs phosphorylation, we evaluated separately the effects of peptide **1** on $VEGF_{165}$-induced VEGFR-1 and VEGFR-2 phosphorylation. As shown in Figure 1A and B, peptide **1** inhibited in a dose-dependent manner both $VEGF_{165}$-induced VEGFR-1 and -2 phosphorylation on HUVEC, with almost total inhibition at 100 μM, a non-negligible effect at 33 and 10 μM, and no inhibition at 3 μM (Figure 1.D). These experiments proved that peptide **1** exhibits an antagonistic effect by acting on VEGFR phosphorylation without significant selectivity.

Inhibitory Effect of Peptide 1 on $VEGF_{165}$-Induced VEGFRs Signaling Pathway. Because of the peptide **1** inhibitory effects on VEGFRs phosphorylation, we examined its downstream activity on the ERK1/2 signaling pathway, particularly involved in the proliferation of endothelial cells.[34] As shown in Figure 1C, peptide **1** led to the inhibition of $VEGF_{165}$-induced ERK1/2 phosphorylation in a dose−effect manner with total inhibition at 100 and 33 μM, partial inhibition at 10 μM, and no effect at 3 μM (Figure 1D). This effect−dose response, obtained on $VEGF_{165}$-induced ERK1/2 phosphorylation, again confirms the antagonist activity of peptide **1**, which is able to inhibit the $VEGF_{165}$ induced signaling pathways.

Peptide Synthesis. In order to identify the amino acids involved in VEGF receptor recognition, we performed an Ala-scan on peptide **1**. We thus generated cyclic 8-mer peptides by sequentially replacing the amino acids that constitute the peptide **1** sequence by an alanine. These peptides were obtained as previously described through solid-phase peptide synthesis using Fmoc chemistry (Scheme 1).[35] After elongation of the peptide chain, the O-allyl protection of the lateral chain of the C-terminal glutamate was removed by treatment with $Pd^{(0)}$,[36] the N-terminal Fmoc was cleaved with piperidine and the peptide cyclized upon addition of the HBTU/HOBt cocktail as coupling reagents. The deprotection of the lateral chains and cleavage from the resin yielded the crude peptide which was then purified by HPLC and characterized by ^1H NMR and mass spectroscopy. In an attempt to improve the yield of this cyclization, we tried to replace the O-allyl protection used in this head to C-terminal side chain cyclization by the Dmab protective group. Another interest of this protective group was that it would preclude the use of the expensive $Pd^{(0)}$ reagents and the extensive washing necessary to eliminate metal traces. Unexpectedly, we obtained the desired peptide as a trace, and the main peptide was identified as the N-terminal tetramethylguanidine-capped peptide. Because the cyclization smoothly proceeded after O-allyl cleavage, we attributed the lack of cyclization to improper aminobenzyl ester collapse during the Dmab deprotection step as already reported.[37] Therefore, the aminobenzyl ester served as a

Table 1. Sequences and Inhibitory Potency of Peptides **1**−**18** on VEGFR-1 Competition Assays

Cyclic vs Linear Peptides					
entry	sequence	activity on VEGFR-1_{ECD} assay at 100 μM[a]	IC_{50} on VEGFR-1_{ECD} assay (μM)[b]	activity on VEGFR-1_{D1-D3} assay at 100 μM[a]	IC_{50} on VEGFR-1_{D1-D3} assay (μM)[b]
1	c[YYDEGLEE]-NH_2	73 ± 7	32 ± 8	84 ± 3	23 ± 2
2	Ac-YYDEGLEE-NH_2	0 ± 3	nd	nd	nd
Ala-Scan Substitutions					
entry	sequence	activity on VEGFR-1_{ECD} assay at 100 μM[a]	IC_{50} on VEGFR-1_{ECD} assay (μM)[b]	activity on VEGFR-1_{D1-D3} assay at 100 μM[a]	IC_{50} on VEGFR-1_{D1-D3} assay (μM)[b]
3	c[**A**YDEGLEE]-NH_2	0 ± 1	nd	4 ± 4	nd
4	c[Y**A**DEGLEE]-NH_2	4 ± 4	nd	3 ± 5	nd
5	c[YY**A**EGLEE]-NH_2	63 ± 10	35 ± 4	77 ± 6	25 ± 1
6	c[YYD**A**GLEE]-NH_2	1 ± 1	nd	1 ± 2	nd
7	c[YYDE**A**LEE]-NH_2	49 ± 12	105 ± 25	46 ± 2	101 ± 18
8	c[YYDEG**A**EE]-NH_2	9 ± 8	nd	9 ± 6	nd
9	c[YYDEGL**A**E]-NH_2	3 ± 1	nd	3 ± 2	nd
Lysine or Phenylalanine Substitutions					
entry	sequence	activity on VEGFR-1_{ECD} assay at 100 μM[a]	IC_{50} on VEGFR-1_{ECD} assay (μM)[b]	activity on VEGFR-1_{D1-D3} assay at 100 μM[a]	IC_{50} on VEGFR-1_{D1-D3} assay (μM)[b]
10	c[YY**K**EGLEE]-NH_2	42 ± 15	nd	45 ± 10	nd
11	c[YY**F**EGLEE]-NH_2	10 ± 8	nd	5 ± 4	nd
12	c[YYDE**K**LEE]-NH_2	41 ± 15	nd	50 ± 11	nd
13	c[YYDE**F**LEE]-NH_2	7 ± 8	nd	3 ± 1	nd
Peptide **1** Optimization Attempts					
entry	sequence	activity on VEGFR-1_{ECD} assay at 100 μM[a]	IC_{50} on VEGFR-1_{ECD} assay (μM)[b]	activity on VEGFR-1_{D1-D3} assay at 100 μM[a]	IC_{50} on VEGFR-1_{D1-D3} assay (μM)[b]
14	c[***d*Y**YDEGLEE]-NH_2	3 ± 12	nd	0 ± 5	nd
15	c[Y**K**DEGLEE]-NH_2	45 ± 3	nd	47 ± 3	nd
Peptide **1** Cycle Size Reduction					
entry	sequence	activity on VEGFR-1_{ECD} assay at 100 μM[a]	IC_{50} on VEGFR-1_{ECD} assay (μM)[b]	activity on VEGFR-1_{D1-D3} assay at 100 μM[a]	IC_{50} on VEGFR-1_{D1-D3} assay (μM)[b]
16	c[YYDEGLE] -NH_2	3 ± 12	nd	0 ± 5	nd
17	c[YYDELE] -NH_2	24 ± 2	nd	1 ± 6	nd
18	c[YYELE] -NH_2	14 ± 2	nd	6 ± 2	nd

[a] Activity corresponds to the percentage of biotinylated $VEGF_{165}$ displaced by the indicated concentration of peptides on VEGFR-1 competition assays. [b] Concentration of peptides that inhibits 50% of the biotinylated $VEGF_{165}$ binding on VEGFR-1_{ECD} and VEGFR-1_{D1-D3}.

transient protection of the lateral chain of the glutamate which allowed the amidine of the HBTU to be transferred to the N-terminus amino group, thus leading to the tetramethylguanidine compound. In the absence of reliable deprotection process of the Dmab protective group and of any improvement of the synthesis, we performed the cyclization as previously described.[23]

Analysis of the Peptide 1 Binding Determinants Involved in VEGFR-1 Interaction. Ala-scan studies are a common way to identify the amino acids which are responsible for the biological activities of a peptide.[38] In order to identify the amino acids of peptide **1** essential for VEGFR-1 binding, we consequently conducted an Ala-scan on it. We synthesized seven derivatives of peptide **1** in which each of the eight residues was replaced by an alanine (peptides **3** to **9** in Table 1B), except the last glutamic acid for which a lateral chain is involved in the cyclization. Their sequences are represented in Table 1B. The inhibitory effect of each of those derivatives on the $VEGF_{165}$ binding to VEGFR-1 was determined by the VEGFR-1_{ECD} competition assay (Table 1B). First, those Ala-scan-peptides were tested at the concentration of 100 μM. In these conditions, only two derivatives, in which, respectively, the aspartic acid in position 3 (D3) or the glycine in position 5 (G5) was replaced by an alanine (peptides **5** and **7**), were still able to disrupt bt$VEGF_{165}$ binding to VEGFR-1_{ECD}. Consequently, the IC_{50} of these two Ala-scan-peptides were determined (Table 1B). Peptides **5** and **7**, respectively, had an IC_{50} of 35 μM and 105 μM on the VEGFR-1_{ECD} assay. These IC_{50} are relatively close to the one exhibited by peptide **1**. The other Ala-scan-peptides, tested at 100 μM, showed no inhibition of the bt$VEGF_{165}$ binding to VEGFR-1_{ECD}, suggesting that the side chains of tyrosines in positions 1 and 2 (Y1, Y2), glutamic acids in positions 4 and 7 (E4, E7), and leucine in position 6 (L6) are involved in the peptide **1** binding to VEGFR-1 or have a stabilizing effect on its biological active conformation. These results were consistent with the assays performed on the VEGFR-1_{D1-D3} (Table 1B). Indeed, in this assay, peptides **5** and **7** inhibited bt$VEGF_{165}$ binding with an IC_{50} of, respectively, 25 and 101 μM, while the other derivatives tested at 100 μM showed no inhibition. All together, those results suggest that D3 and G5 are not essential for peptide **1** binding to VEGFR-1 and that the peptides **5** and **7** target the $VEGF_{165}$ binding sites on VEGFR-1 in the same way peptide **1** does.

Effect of Ala-Scan Peptides on $VEGF_{165}$-Induced VEGFRs Phosphorylation. To determine the specificity of peptides **3**−**9**, we assessed their effects on $VEGF_{165}$-induced

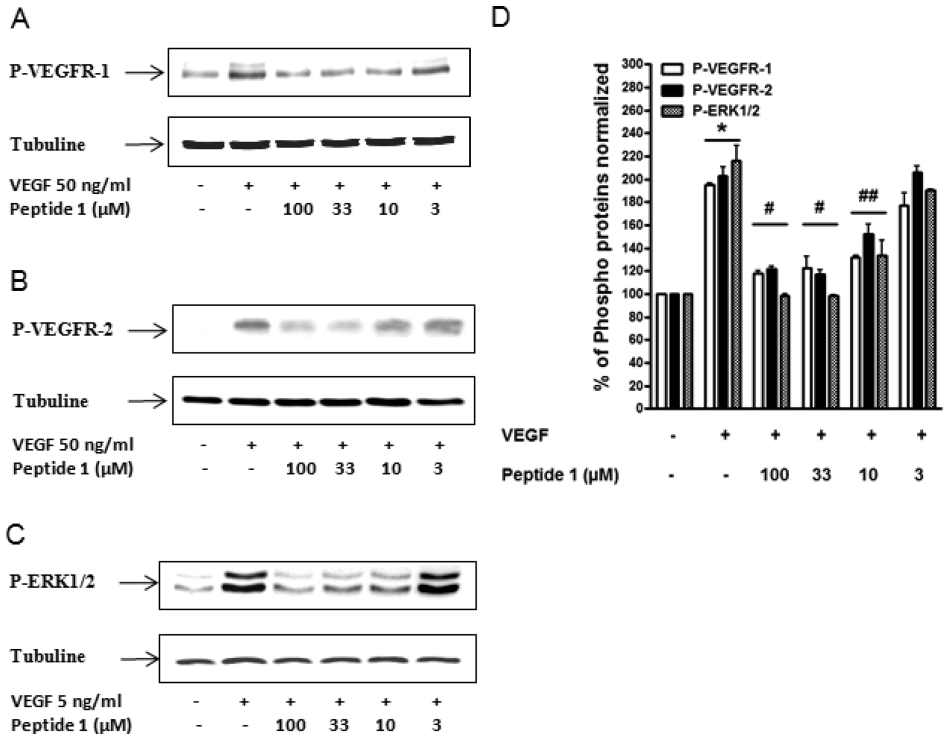

Figure 1. Inhibition of $VEGF_{165}$-induced VEGFR-1, VEGFR-2, and ERK1/2 phosphorylations by peptide **1**. Starved HUVEC were incubated with peptide **1** at the indicated concentration over a period of 1 h and then stimulated by $VEGF_{165}$ 50 ng/mL (1.3 nM) for 5 min for VEGFRs phosphorylation or by $VEGF_{165}$ 5 ng/mL (131 pM) for 15 min for ERK1/2 phosphorylation. A. Western Blot performed with antiphospho VEGFR-1 and anti-α-tubulin representative of three independent experiments. B. Western blot performed with antiphospho VEGFR-2 and anti-α-tubulin representative of three independent experiments. C. Western blot performed with antiphospho ERK1/2 and anti-α-tubulin representative of three independent experiments. D. Relative optical densities of the bands in arbitrary units. All results are expressed as mean ± SD. Control without $VEGF_{165}$ is considered as 100%. * $p < 0.0001$ vs the group without $VEGF_{165}$ and # $p < 0.0001$ and ## $p < 0.005$ vs the group with $VEGF_{165}$.

Scheme 1. General Procedure for the Synthesis of Peptides **1**−**18**

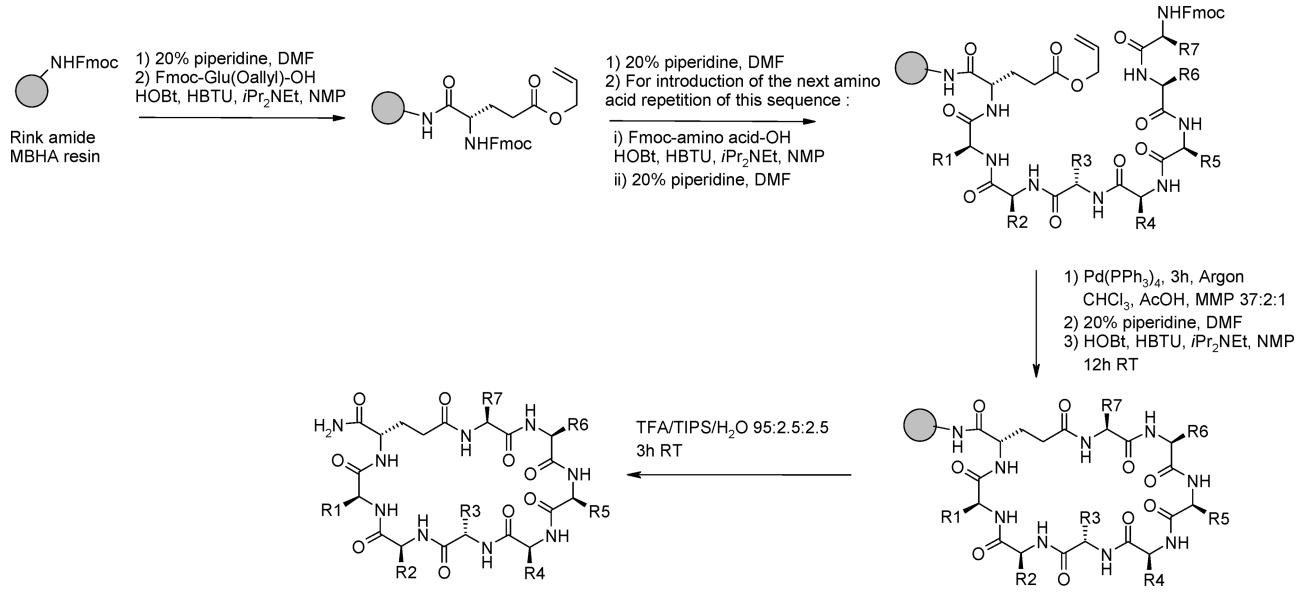

VEGFRs phosphorylation on HUVEC (Figure 2). Tested at 100 μM, only peptides **5** and **7** inhibited $VEGF_{165}$-induced VEGFR-1 and -2 phosphorylation by a factor of 3. The other Ala-scan peptides showed no inhibition of $VEGF_{165}$-induced VEGFRs phosphorylation. These results demonstrated that neither D3 nor G5 is necessary for peptide **1** binding to VEGFR-1 or to VEGFR-2. They also revealed that the corresponding peptides **5** (D3A) and **7** (G5A) exhibit antagonist activities through inhibition of both VEGFR-1 and VEGFR-2 phosphorylation as for peptide **1**.

Ala-Scan-Derived Peptides. Since residues D3 and G5 of peptide **1** are apparently not required for its binding to VEGFRs and for its antagonist activity, we separately replaced these two amino acids by a lysine (K) or a phenylalanine (F).

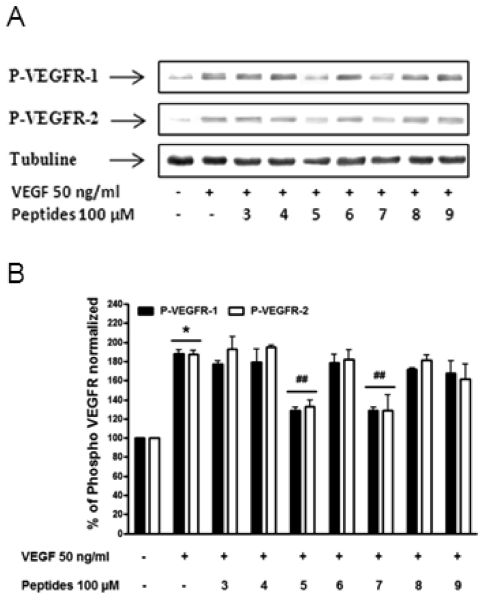

Figure 2. Inhibition of $VEGF_{165}$-induced VEGFR-1 and VEGFR-2 phosphorylation by Ala-scan-derived peptides. Starved HUVEC were incubated with peptides at 100 μM over a period of 1 h and then stimulated by $VEGF_{165}$ 50 ng/mL (1.3 nM) for 5 min. A. Western blot performed with antiphospho VEGFR-1, antiphospho VEGFR-2, or anti-α-tubulin is representative of three independent experiments. B. Relative optical density of the bands in arbitrary units. Control without $VEGF_{165}$ is considered as 100%. Results are expressed as mean ± SD. * $p < 0.0001$ vs the group without $VEGF_{165}$ and ## $p < 0.005$ vs the group with $VEGF_{165}$.

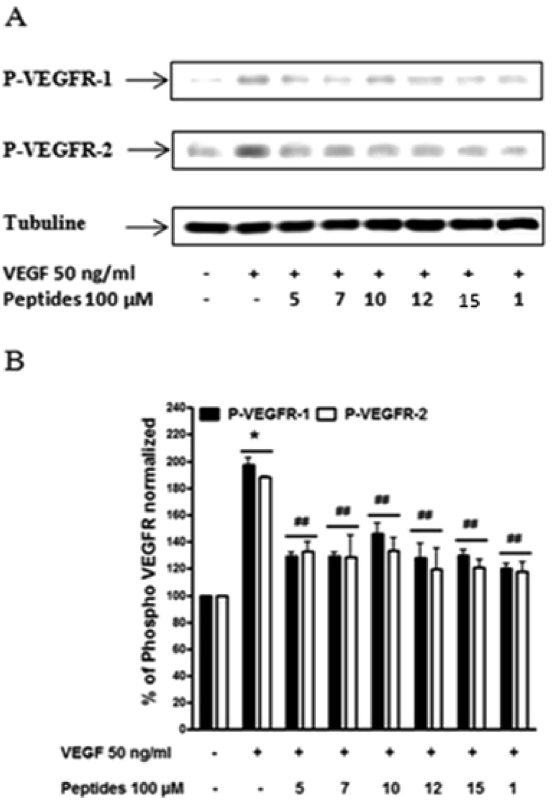

Figure 3. Inhibition of $VEGF_{165}$-induced VEGFRs phosphorylation by Ala-scan-derived peptides. Starved HUVEC were incubated with peptides at 100 μM over a period of 1 h and then stimulated by $VEGF_{165}$ 50 ng/mL (1.3 nM) for 5 min. A. Western blots performed with antiphospho VEGFR-1, antiphospho VEGFR-2, or anti-α-tubulin are representative of three independent experiments. B. Relative optical density of the bands in arbitrary units. Control without $VEGF_{165}$ is considered as 100%. Results are expressed as mean ± SD. * $p < 0.0001$ vs the group without $VEGF_{165}$ and ## $p < 0.005$ vs the group with $VEGF_{165}$.

The corresponding peptides were synthesized and respectively called peptides **10** (D3K), **11** (D3F), **12** (G5K), and **13** (G5F). They were then tested at 100 μM on the VEGFR-1 competition assays and compared to peptides **1**, **5** (D3A), and **7** (G5A) as controls. Results are shown in Table 1. On $VEGFR\text{-}1_{ECD}$ competition assay, peptide **1** showed 73% of inhibition. At 100 μM, the inhibition of the analogues of peptide **1**, in which either D3 or G5 was replaced by an alanine, were, respectively, of 63% and 49% and in the case of the replacement by a lysine of 42% and 41%. The peptides **10** and **12** thus bear an inhibition of the same magnitude as their corresponding Ala-scan peptides **5** and **7**. On the other hand, the replacement of either D3 or G5 by a phenylalanine induced a total loss of inhibition. The same results were obtained at 100 μM on the $VEGFR\text{-}1_{D1\text{-}D3}$ competition assay in which peptide **1** showed an inhibition of 84%. Indeed, this inhibition persisted when D3 was mutated by an alanine (77%) or by a lysine (45%) and when G5 was replaced by an alanine (46%) or a lysine (50%), whereas the replacement by a phenylalanine completely abolished it. Peptides **10** and **12** were then evaluated on $VEGF_{165}$-induced VEGFRs phosphorylation (Figure 3). Tested at 100 μM, these two peptides almost completely inhibited both VEGFR-1 and -2 phosphorylations in response to $VEGF_{165}$, as the peptide controls **1**, **5**, and **7** did.

Peptide 1 Optimization Attempts. On the basis of previous modeling data of peptide **1** docked into VEGFR-1 domain 2 ($VEGFR\text{-}1_{D2}$),[23] we modified different amino acids of its sequence. In some cases, it is described that the configuration change of one amino acid in a peptide can increase its affinity for its target.[39] Considering this, we started by modifying the first tyrosine residue (Y1), changing its configuration to D-tyrosine (peptide **14**). Unfortunately, peptide **14** did not inhibit at 100 μM $btVEGF_{165}$ binding to $VEGFR\text{-}1_{ECD}$ and $VEGFR\text{-}1_{D1\text{-}D3}$ (Table 1D). We then replaced Y2 by a lysine enabled to mimic, in terms of interaction, the hydrophobicity of the tyrosine aromatic cycle through its side chain and the tyrosine OH group through its NH_2 function (peptide **15**). On the VEGFR-1 assays, peptide **15**, tested at 100 μM, inhibited approximately 50% of $btVEGF_{165}$ binding to $VEGFR\text{-}1_{ECD}$ and $VEGFR\text{-}1_{D1\text{-}D3}$ (Table 1D).

We finally studied the influence of peptide **1** cycle size on its activity. Since D3 and G5 of peptide **1** are not essential for its binding to VEGFRs, we synthesized three peptides, each corresponding to peptide **1**: without the glutamic acid in position 8 (E8) (peptide **16**), without G5 and E8 (peptide **17**), and without D3, E8, and G5 (peptide **18**). Performed on the VEGFR-1 competition assays, each of these cycle size-reduced peptides showed no inhibition of $btVEGF_{165}$ binding to VEGFR-1 (Table 1E), suggesting the critical conformation displayed by the peptide **1** cycle size.

NMR Mapping Studies of the Peptides 1 and 5 Binding Site on $VEGFR\text{-}1_{D2}$. Upon progressive additions of the unlabeled peptides **1** and **5** to ^{15}N-labeled $VEGFR\text{-}1_{D2}$, we observed continuous changes in ^1H and ^{15}N chemical shifts for several signals in the $^1H-^{15}N$ HSQC spectra of the $VEGFR\text{-}1_{D2}$. For each peptide, $\Delta\delta HN_{av}$ (Experimental Section) of every amino acid at 2:1 peptide/protein ratio was reported (Figure 4) and residues having $\Delta\delta HN_{av} \geq 0.2$ ppm mapped onto the NMR

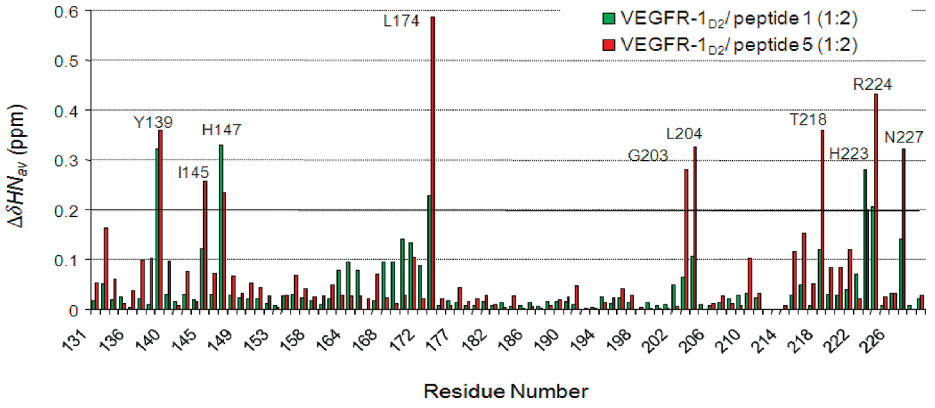

Figure 4. Histogram of the variation in chemical shift [$\Delta\delta$HN(ppm) = [(0.17ΔN)2 + (ΔH)2]1/2] observed in $^{1}H-^{15}N$ HSQC spectra of VEGFR-1_{D2} in the presence of 2 equiv of peptide **1** (in green) and in the presence of 2 equiv of peptide **5** (in red). The amino acids that undergo a significant chemical shift change [$\Delta\delta$(ppm) $\geq$ 0.2] upon formation of the VEGFR-1_{D2}/peptide complex were highlighted by the threshold.

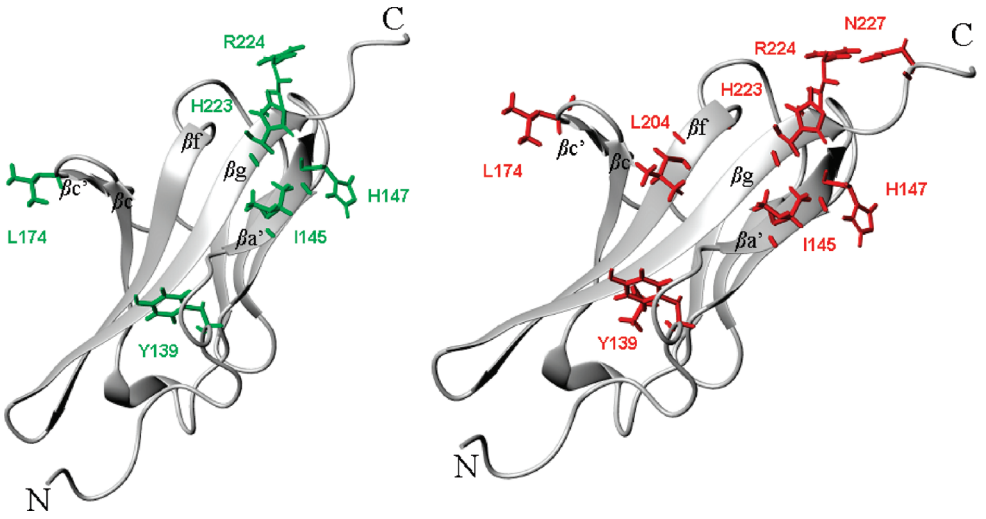

Figure 5. Ribbon model of the free VEGFR-1_{D2} NMR structure. The amino acids that undergo significant chemical shift changes upon formation of the VEGFR-1_{D2}/peptide **1** complex (in green) and of the VEGFR-1_{D2}/peptide **5** complex (in red) were mapped onto a model of the NMR structure of the VEGFR-1_{D2}.

solution structure of the VEGFR-1_{D2} (Figure 5). Peptides **1** and **5** share a common binding site on the VEGFR-1_{D2}, consisting of portions of βa′ strand (H^{147}), βg strand (H^{223} and R^{224}), of the loop between βc and βc′ strands (L^{174}) and of the N-terminal region (Y^{139}). However, peptide **5** binding affects a larger VEGFR-1_{D2} surface, also including I^{145} from βa′ strand, βf strand (G^{203} and L^{204}), T^{218} in βg strand, and the *C*-terminal residues N^{227}.

Pull-Down Assay. The replacement by a lysine of either Y2, D3, or G5 in peptide **1** gave us the opportunity to graft peptides **10**, **12**, and **15** onto sepharose beads, in order to verify whether or not it would impair the recognition properties of the peptides. Thus, peptides **10**, **12**, and **15** immobilized on CNBr-activated sepharose were incubated with recombinant VEGFR-1_{ECD}, VEGFR-2_{ECD}, or VEGFR-1_{D2}.[40] The retained VEGFRs were analyzed by Western blot. As shown in Figure 6, only peptides **12** and **15** immobilized on sepharose were able to interact with VEGFR-1_{ECD}, VEGFR-2_{ECD}, and VEGFR-1_{D2}, roughly with three times more retained receptors than with the control.

Discussion

On the basis of the crystallographic structure of $VEGF_{8-109}$ in complex with VEGFR-1_{D2} resolved in 1997 by Wiesmann et al.,[25] we previously reported cyclic peptides simultaneously mimicking two epitopes of the $VEGF_{165}$ involved in the VEGFR-1 interaction: the α-helix 16−27 (KFMDVYQRSYCH) and the loop 61−68 connecting β3 and β4 strands (CN**DEGLE**C) which adopts a pseudocyclic structure.[22] The novelty and the challenge of such cyclic peptides are due to the fact that they mimic two discontinuous epitopes of the $VEGF_{165}$, close in the protein's spatial structure but relatively distant regarding its amino acid sequence.[41] One of these cyclic peptides, named peptide **1** in this work, which has the sequence c[**YYDEGLEE**]-NH_2, was shown to prevent $VEGF_{165}$ binding to VEGFR-1 and to exhibit antagonist activities on endothelial cells.[23] Although satisfactory, these preliminary results should be further explored. Indeed, only Y1 and L6 were identified as being essential for receptor binding. Moreover, the cellular effects of peptide **1** were studied at a single dose without considering its specificity for the VEGF receptors. Last, in order to graft the peptide to cyclen for future use in medical imaging, it was necessary to determine which amino acid could be replaced by a lysine without loss of affinity for the target.

First, in order to determine the prominence of the peptide **1** cyclic form, we synthesized its linear analogue (peptide **2**). After evaluation on the VEGFR-1_{ECD} assay, the peptide **2** showed no inhibition of bt$VEGF_{165}$ binding to VEGFR-1_{ECD}

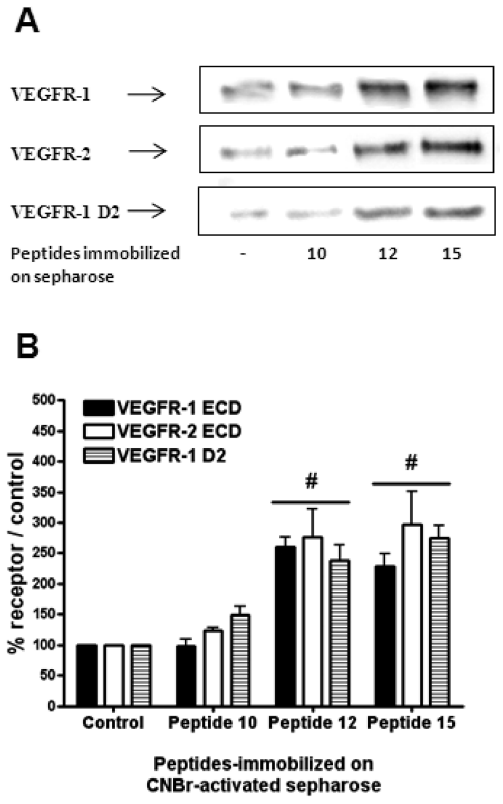

Figure 6. VEGFRs pull-down assay on peptides immobilized on CNBr-activated sepharose. A. Western Blot performed with anti-VEGFR-1 and antiphospho VEGFR-2 representative of three independent experiments. B. Relative optical density of the bands in arbitrary units. Control without peptide-immobilized on CNBr-activated sepharose is considered as 100%. Results are expressed as mean ± SD. # $p < 0.0001$ vs the group control.

(Table 1A). This result confirms the requirement of a cyclic structure which by reducing the conformational possibilities of the peptide **1** allows it to mimic the pseudocyclic region C61−C68 and therefore to inhibit the $VEGF_{165}$/VEGFR-1 interaction in the competition assays.

Then, we investigated whether peptide **1** inhibits $VEGF_{165}$ binding to VEGFR-1 by interfering with the $VEGF_{165}$ binding sites. We assessed its ability to inhibit $btVEGF_{165}$ binding to VEGFR-$1_{D1\text{-}D3}$ entailing the essential domains for $VEGF_{165}$ high-affinity binding. Because peptide **1** inhibited $btVEGF_{165}$ binding to VEGFR-$1_{D1\text{-}D3}$ with an IC_{50} of 23 μM (Table 1A), close to the one obtained on VEGFR-1_{ECD}, it implies that peptide **1** would target $VEGF_{165}$ binding sites on VEGFR-1. Combined to its inhibition of $VEGF_{165}$-induced VEGFR-1 phosphorylation on endothelial cells (Figure 1), this result suggests that peptide **1** exhibits antagonist activity by interfering with $VEGF_{165}$ binding sites but not with other sites like the ones involved in the VEGFR-1 dimerization.[42,43]

Because peptide **1** was designed as a VEGF mimic, we were expecting that this peptide would interact with VEGFR-1_{D2} in the same way as observed for VEGF in the reported 3D-structure.[25] The VEGFR-1_{D2} amino acids involved in the VEGF binding are the following ones: Y139, E141, I142, P143, I145, H147, K171, F172, P173, Y199, K200, I202, L204, N219, L221, H223, and R224.[44] Interestingly, the NMR study data showed that the VEGFR-1_{D2} residues involved in the peptides **1** and **5** recognition (Y139, H147, L174, G203, L204, T218, H223, R224) are almost all included in those listed before. These results emphasize that these peptides share the same binding region as VEGF, thus explaining their antagonist activity. Moreover, at least a part of the VEGFR-1_{D2} binding site should entail the following amino acids F172, P173, Y199, K200, I202, L204, L221, and R224 interacting with the Y21, Y25, D63, G65, and L66 of VEGF, which are mimicked in peptide **1** by Y1, Y2, D3, G5, and L6. In addition, as a result of the molecular modeling study, we have already reported that two supplementary interactions with K171 and H223 could be awaited.[23] The NMR study of the complex formed through association of peptide **1** with the VEGFR-1_{D2} highlighted a slightly different binding epitope containing the H223 and R224 and the more distant Y139, H147, and L174 amino acids. It is noteworthy that all these amino acids except L174 are part of the VEGF binding area, thus confirming that peptide **1** interacts in a similar way as VEGF. Furthermore as pointed out in the NMR study of unbounded VEGFR-1_{D2}, L174, and Y139 have a high mobility; consequently, we could not exclude that the peptide binding to the receptor could indirectly influence their conformation.[44] In order to refine these results, we used a peptide issued from the Ala-scan study, namely, peptide **5** which had the same affinity for the VEGFR-$1_{D1\text{-}D3}$ as peptide **1** (Table 1B). The peptide **5** interacted with the same set of amino acids covered by peptide **1**, but also affected a larger VEGFR-1_{D2} surface, which included I145, G203, L204, and N227. This result confirms that the two peptides share a common binding epitope. Nevertheless, further supplementary experiments are necessary to fully understand how these peptides interact with the receptor. A study aiming at cocrystallizing the peptides with the VEGFR-1_{D2} is underway.

The region C61−C68 of the $VEGF_{165}$ was suggested to be more involved in the $VEGF_{165}$ binding to VEGFR-1 than VEGFR-2 according to mutagenesis data.[31] Consequently, we expected peptide **1** to exhibit more specificity for VEGFR-1 than for VEGFR-2. However, experiments performed on $VEGF_{165}$-induced VEGFRs phosphorylation on endothelial cells showed that peptide **1** inhibits both VEGFR-1 and -2 phosphorylations without significant specificity (Figure 1). Although this result could appear surprising, mutagenesis data could explain it. First, E64 (E4 in peptide **1**) contained in the region C61−C68 seems to be involved into $VEGF_{165}$ binding to VEGFR-2, since its replacement by an alanine decreases $VEGF_{165}$ affinity for VEGFR-2 by a factor 10.[27,28] Second, peptide **1** also mimics two aromatic residues of the α-helix (Y21 and Y25 of the $VEGF_{165}$), which were suggested to be involved both in the $VEGF_{165}$ binding to VEGFR-1 and VEGFR-2.[29] These structural considerations based on mutagenesis data were confirmed by Alitalo and co-workers who determined very recently the crystal structure of the complex VEGF-C/VEGFR-2, which highlighted that the two epitopes mimicked by peptide **1** and conserved in the VEGF-C are involved in the VEGFR-2 interaction.[45] Third, we showed that peptide **1** inhibits activation of $VEGF_{165}$-induced ERK1/2 signaling pathway involved in endothelial cells proliferation (Figure 1C). Up to now, a number of studies have demonstrated that VEGFR-2 is the main mediator of $VEGF_{165}$ effects on endothelial cells.[46,47] On the other hand, VEGFR-1 signaling pathway in endothelial cells is not clearly established yet due to its low level of phosphorylation in response to $VEGF_{165}$.[48,49] Thus, inhibition of the $VEGF_{165}$-induced ERK1/2 activation by peptide **1** may, for an important part, stem from its antagonist effect on VEGFR-2 (Figure 1C).

Among $VEGF_{165}$ residues mimicked by peptide **1**, mutagenesis studies revealed that Y21, Y25, D63, E64, and L66

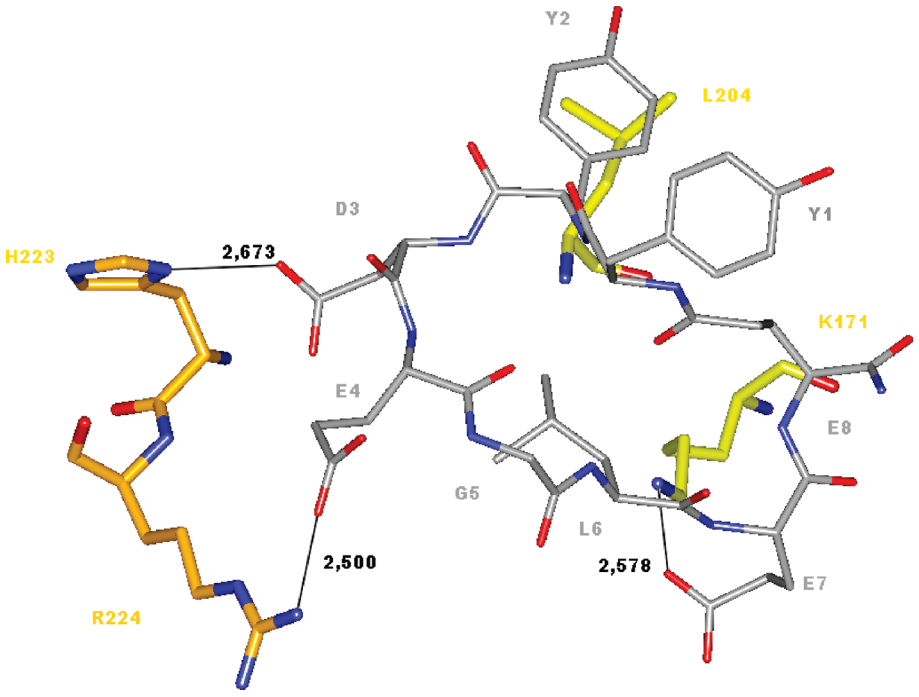

Figure 7. Hydrogen bond network within the complex formed between VEGFR-1 and peptide **1**. Model obtained after docking and minimization of peptide **1** 3D structure into the VEGFR-1_{D2}.[23] The VEGFR-1_{D2} amino acid side chains involved in hydrogen bonds (K171, H223, and R224) in stick representation are colored in yellow. The peptide **1**, in stick representation, is colored gray and shows the amino acids implicated in hydrogen bonds (D3, E4, and E7).

appear to be among the most involved in the $VEGF_{165}$ interaction with VEGFR-1.[29,50] In order to compare the peptide **1** sequence with the corresponding amino acids in $VEGF_{165}$, peptide **1** can be written with the following numbering: c(Y25−Y21-D63-E64-G65-L66-E67-E) (amino acid numbers correspond to the $VEGF_{165}$ sequence). To determine the peptide **1** amino acids involved in the VEGFR-1 interaction, we performed an Ala-scan by replacing each residue by an alanine. Interestingly, the Ala-scan results on VEGFR-1 competition assays confirmed the prevalence of Y25, Y21, E64, and L66 in the $VEGF_{165}$ binding to VEGFR-1 (Table 1B). Unexpectedly, D3 which corresponds to D63 in the VEGF sequence, did not seem to be essential for the VEGFR-1 binding; although in the crystallographic structure of the $VEGF_{8-109}$/VEGFR-1_{D2} complex, D63 forms a salt bridge with R224 of the VEGFR-1_{D2}.[25] Nevertheless, previous modeling data of peptide **1** docked into the VEGFR-1_{D2} revealed that E4 could replace D3 for the establishment of the ionic bond with R224 (Figure 7).[23] Indeed, these modeling data seemed to be reinforced both by the common affinity of peptide **5** (D3A) and peptide **1** for VEGFR-1 and by the complete loss of activity for VEGFR-1 exhibited by peptide **6** (E4A) (Table 1B). Combined together, the Ala-scan experiments and the NMR results corroborate with the ones from structural and mutagenesis of the VEGF/VEGFR-1 interaction studies and prove that peptide **1** both targets the VEGF interaction region on VEGFR-1 and mimics at least a part of the $VEGF_{165}$ epitopes.

Then, we investigated whether peptides from Ala-scan exhibited specificity toward VEGFR-1 and VEGFR-2. The Ala-scan-peptides, tested at 100 μM, on $VEGF_{165}$-induced VEGFR-1 phosphorylation on HUVEC showed that only peptides **5** and **7** inhibit VEGFR-1 phosphorylation (Figures 2 and 3). Thus, these results confirm the idea that D3 and G5 are not necessary for peptide **1** binding to VEGFR-1. Since the alanine introduction can potentially disturb the overall conformation of peptide **1**, it was supposed that each derivate would have a different specificity for VEGFR-1 and VEGFR-2. Nevertheless, only peptides **5** and **7** also inhibit $VEGF_{165}$-induced VEGFR-2 phosphorylation at 100 μM (Figures 2 and 3). The nonspecificity exhibited by peptides **5** and **7** could be explained by the same reasons described above for peptide **1**.

After showing that D3 and G5 of peptide **1** were not be required for its binding to VEGFR and its antagonist activity, we replaced separately these two residues by a phenylalanine (respectively peptides **11** and **13**) or a lysine (respectively peptides **10** and **12**). Because these introductions could affect the peptides conformation compared to the one of peptide **1**, we first evaluated their ability to inhibit bt$VEGF_{165}$ binding to VEGFR-1 (Table 1. C). Tested at 100 μM, peptides **11** and **13** were unable to inhibit bt$VEGF_{165}$ to VEGFR-1 suggesting that the phenylalanine introduction was likely to destabilize the peptide conformation. Contrary to the phenylalanine introduction, the lysine one does not significantly affect the peptide conformation, since peptides **10** and **12** almost exhibited the same magnitude of inhibition as peptide **1**. Furthermore, peptides **10** and **12**, while tested at 100 μM, inhibited $VEGF_{165}$-induced VEGFR-1 and VEGFR-2 phosphorylation on HUVEC (Figure 3). Considered together, these two results suggest that lysine introduction instead of D3 or G5 does not affect the inhibitory and antagonist properties of peptide **1** on VEGFR-1 and -2.

Next, in order to increase the peptide **1** activity, we performed optimization attempts of this peptide by reducing its cycle size. In accordance with the Ala-scan results, peptides **16**, **17**, and **18** were synthesized. The effects of these peptides on VEGFR-1 competition assays revealed that the reduction of the cycle size induced a total loss of activity (Table 1E), indicating that an 8-mer cyclic peptide is of optimal size for

interacting with the VEGFR-1 as suggested by the model of peptide **1** docked onto VEGFR-1_{D2}.[23] On the basis of this model, we also deduced that, in peptide **1**, the tyrosine in position 1 (Y1) was not suitable to interact with VEGFR-1 (Figure 7). Thus, we replaced an L-Y1 (peptide **1**) by a D-Y1 (peptide **14**). Unfortunately, this manipulation did not produce the results expected since peptide **14** inhibited bt$VEGF_{165}$ binding neither to VEGFR-1_{ECD} nor to VEGFR-$1_{D1\text{-}D3}$ at 100 μM (Table 1. D). A probable cause of this result may come from conformational changes induced by D-tyrosine. Second, still according to these previous modeling data, the tyrosine in position 2 (Y2) would interact with VEGFR-1_{D2} through hydrophobic bonds of its aromatic cycle and hydrogen bond of its OH function (Figure 7). Thus, we replaced this tyrosine by a lysine which side chain respects these described interaction properties (peptide **15**). This peptide, tested at 100 μM, inhibited 50% of bt$VEGF_{165}$ binding to VEGFR-1_{ECD} and VEGFR-$1_{D1\text{-}D3}$ assays (Table 1D). Moreover, peptide **15** almost completely inhibited both $VEGF_{165}$-induced VEGFR-1 and VEGFR-2 phosphorylation at 100 μM (Figure 3).

Thus, replacement of Y2, D3, and G5 by a lysine led to three different peptides **10**, **12**, and **15**, capable of retaining a sufficient affinity for the VEGFRs and of remaining active during cellular assays. In order to test the ability of the peptides to conserve their affinity for the VEGFRs even when they are grafted to a bulky component, we used sepharose beads as cyclen surrogates. Indeed, introduction of a cyclen in a peptide entity is not an easy task, while grafting onto sepharose beads is a well-defined and straightforward approach for identifying binding partners.[51] Peptides **10**, **12**, and **15** were consequently immobilized on CNBr-activated sepharose through the amino function of the lysine, and the obtained constructs were used in a pull-down assay (Figure 6). Then, peptides were incubated with recombinant VEGFR-1_{ECD}, recombinant VEGFR-2_{ECD}, or VEGFR-1_{D2}.[40] Finally, the retained VEGFRs were revealed by Western blot. In this pull-down assay, only peptides **12** and **15** were able to trap both VEGFR-1_{ECD} and VEGFR-2_{ECD}, which corroborates their ability to interact with both receptors. In particular, peptides **12** and **15** interacted with VEGFR-1_{D2} highlighting their potential binding to the D2 region determined by NMR. Unexpectedly, peptide **10** immobilized on CNBr-activated sepharose did not show the same binding properties with no receptors retained which could be explained by conformational changes induced by the binding of the peptide to the beads.

Conclusion

Overall, these data strongly support the need for further development of these peptides as tools for studying angiogenesis-related diseases. Indeed, this work has allowed us to confirm that these peptides effectively bind to the VEGF receptors at the same epitope as $VEGF_{165}$. In addition, they inhibit the VEGF binding to its receptors, thus resulting in the inhibition of the transduction pathways initiated by $VEGF_{165}$. Furthermore, modification of the peptides through addition of cyclen on the lateral chains of lysine should constitute the basis for the design of new probes for medical imaging purposes. Moreover, lysine containing peptide could also be used to explore the surface of the receptor by grafting different chemical groups to the lysine side chain in order to obtain optimized antagonists.

Experimental Section

Chemistry. Reagents. All amino acids, coupling reagents, and resin were purchased from Novabiochem. The amino acids are N^{α}-Fmoc protected and their lateral chains were protected as follows: Asp(O-*t*-Bu), Asp(O-All), Glu(O-*t*-Bu), Glu(O-All), Tyr(O-*t*-Bu), and Lys(N-Boc). All analytical-grade solvents were commercially obtained and used without further purification. Tetrakis(triphenyl)palladium (0) was purchased from Sigma-Aldrich at a purity of 99% and used without purification.

General Procedure for Peptide Synthesis. All peptides were synthesized by solid-phase peptide synthesis on an Applied Biosystem 433A synthesizer at 0.25 mmol scale using Fmoc chemistry and MBHA rink amide resin (0.68 mmol/g: 0.36 g) as support. Coupling reactions were performed using Fmoc amino acids (4 equiv related to the resin), activated with HBTU (4 equiv) and HOBt (4 equiv) in the presence of DIPEA (8 equiv) for 1 h. After each coupling step, Fmoc removal was effected by treating the resin with 20% piperidine in NMP for 15 min, except for the last amino acid, which was left protected. After completion of the chain elongation the O-allyl group was cleaved by addition of tetrakis(triphenyl) palladium (0) following a standard procedure. The N-terminal part was released by cleavage of the Fmoc with piperidine and the resin carefully washed with NMP. The cyclization was realized overnight by addition of a mixture composed of 8 mL NMP, 0.25 mL 2 M DIPEA, and 0.25 mL 100 mM HBTU to the resin. After washing steps with NMP and DCM, the deprotection and cleavage of the peptide from the resin was done by treatment with 10 mL of TFA/water/TIPS: 95/2.5/2.5 for 3 h at room temperature. After removal of the resin through filtration, the filtrate was concentrated in vacuo and precipitated with cold diethyl ether. The precipitate was collected by filtration affording the crude peptide in nearly quantitative yields with a purity of about 70%. The crude peptides were purified by semipreparative HPLC on Vydac C18 column (5 μm, 10 $\times$ 250 mm) using a gradient program beginning with 10% B for 10 min and rising to 90% B in 80 min at a flow rate of 2 mL/min (solvent A is water with 0.1% TFA, solvent B is 70% acetonitrile aqueous solution with 0.09% TFA). The products were detected at 214 and 254 nm, collected, and analyzed by HPLC using a Vydac C18 column (5 μm, 2.5 $\times$ 250 mm). Pure fractions were pooled and lyophilized to yield the final peptides as white solid with at least 95% purity.

Peptide 1 c[YYDEGLEE]-NH_2. Yield: 25 mg, 10%. ^{1}H NMR (DMSO-d_6): 0.84 (d, J = 6.5 Hz, 3H, CH_3), 0.88 (d, J = 6.5 Hz, 3H, CH_3), 1.51 (m, 2H), 1.64 (m, 1H), 1.85 (m, 3H), 2.02 (m, 3H), 2.25 (m, 6H), 2.64 (m, 2H), 2.84 (m, 3H), 2.93 (m, 1H), 3.57 (dd, J = 16.5 Hz, J = 5 Hz, 1H), 3.80 (dd, J = 16.5 Hz, J = 5 Hz, 1H), 4.09 (m, 3H), 4.16 (m, 2H), 4.25 (m, 1H), 4.34 (m, 1H), 6.63 (d, J = 8.5 Hz, 2H), 6.66 (d, J = 8.5 Hz, 2H), 6.98 (d, J = 8.5 Hz, 2H), 6.99 (s, 1H, $CONH_2$), 7.01 (d, J = 8.5 Hz, 2H), 7.02 (s, 1H, $CONH_2$), 7.60 (d, J = 9 Hz, 1H, NH), 7.64 (d, J = 9 Hz, 1H, NH), 7.8 (m, 2H, NH), 7.92 (m, 2H, NH), 8.21 (bs, 1H, NH), 8.41 (d, J = 9 Hz, 1H, NH), 9.14 (s, 1H, OH), 9.17 (s, 1H, OH), 12.14 (bs, 3H, COOH). MS m/z calcd for $C_{45}H_{59}N_9O_{17}$ 997; found 998.2 [M+H$^+$]. Rt = 13.2 min (10−90% of solvent B in 30 min, purity 96%).

Peptide 2 Ac-YYDEGLEE-NH_2. Yield 42 mg, 16%. ^{1}H NMR (DMSO-d_6): 0.83 (d, J = 6.5 Hz, 3H, CH_3), 0.88 (d, J = 6.5 Hz, 3H, CH_3), 1.44 (m, 2H), 1.58 (m, 1H), 1.72 (s, 3H), 1.76 (m, 3H), 1.91 (m, 3H), 2.20 (m, 2H), 2.26 (m, 4H), 2.51 (m, 1H), 2.68 (m, 2H), 2.74 (m, 1H), 2.80 (m, 1H), 2.91 (m, 1H), 3.57 (dd, J = 16.5 Hz, J = 5.5 Hz, 1H), 3.80 (dd, J = 16.5 Hz, J = 5.5 Hz, 1H), 4.18 (m, 2H), 4.24 (m, 1H), 4.34 (m, 2H), 4.40 (m,1H), 4.55 (q, J = 7.3 Hz, 1H), 6.60 (d, J = 8.5 Hz, 2H), 6.62 (d, J = 8.5 Hz, 2H), 6.96 (d, J = 8.5 Hz, 2H), 7.00 (d, J = 8.5 Hz, 2H), 7.06 (s, 1H, $CONH_2$), 7.27 (s, 1H, $CONH_2$), 7.72 (d, J = 7.4 Hz, 1H, NH), 7.87 (m, 3H, NH), 8.03 (d, J = 7 Hz, 1H, NH), 8.05 (t, J = 5.5 Hz, 1H, NH), 8.11 (d, J = 7.7 Hz, 1H, NH), 8.33 (d, J = 7.7 Hz, 1H, NH),

9.10 (s, 2H, OH), 9.17 (s, 1H, OH), 12.14 (bs, 3H, COOH). MS m/z calcd for $C_{47}H_{63}N_9O_{19}$ 1057; found 1058.2 [M+H$^+$]. Rt = 12.9 min (30−60% of solvent B in 20 min, purity 95%).

Peptide 3 c[AYDEGLEE]-NH$_2$. Yield: 6.1 mg, 2.7%. ^{1}H NMR (DMSO-d_6): 0.83 (d, J = 6.5 Hz, 3H, CH$_3$), 0.87 (d, J = 6.5 Hz, 3H, CH$_3$), 1.12 (d, J = 7.0 Hz, 3H, CH$_3$), 1.47 (m, 2H), 1.61 (m, 1H), 1.69 (m, 1H), 1.83 (m, 2H), 1.97 (m,3H), 2.12 (m, 2H), 2.27 (m, 4H), 2.64 (m, 1H), 2.88 (m, 3H), 3.56 (dd, J = 16.5 Hz, J = 5 Hz, 1H), 3.77 (dd, J = 16.5 Hz, J = 5 Hz, 1H), 4.02 (m, 1H), 4.07 (m, 2H), 4.20 (m, 4H), 6.64 (d, J = 9 Hz, 2H), 6.67 (d, J = 9 Hz, 2H), 7.03 (s, 1H, CONH$_2$), 7.06 (s, 1H, CONH$_2$), 7.67 (m, 4H, NH), 7.95 (m, 2H, NH), 8.32 (d, J = 4.5 Hz, 1H, NH), 8.35 (d, J = 7 Hz, 1H, NH), 9.15 (s, 1H, OH), 12.05 (bs, 2H, COOH), 12.30 (bs, 1H, COOH). MS m/z calcd for $C_{39}H_{55}N_9O_{16}$ 905; found 906.3 [M+H$^+$]. Rt = 6.7 min (20−50% of solvent B in 16 min, purity 93%).

Peptide 4 c[YADEGLEE]-NH$_2$. Yield: 16 mg 8%. ^{1}H NMR (DMSO-d_6): 0.84 (d, J = 6 Hz, 3H, CH$_3$), 0.88 (d, J = 6 Hz, 3H, CH$_3$), 1.24 (d, J = 6.5 Hz, 3H, CH$_3$), 1.50 (m, 2H), 1.67 (m, 2H), 1.86 (m, 2H), 2.02 (m,3H), 2.24 (m, 6H), 2.58 (m, 1H), 2.75 (m, 2H), 2.69 (m, 1H), 3.58 (dd, J = 16.5 Hz, J = 5 Hz, 1H), 3.80 (dd, J = 16.5 Hz, J = 5 Hz, 1H), 3.97 (m, 1H), 4.05 (m, 2H), 4.16 (m, 2H), 4.26 (m, 1H), 4.37 (m, 1H), 6.64 (d, J = 9 Hz, 2H), 7.01 (m, 3H), 7.03 (s, 1H, CONH$_2$), 7.60 (m, 2H, NH), 7.76 (m, 2H, NH), 7.91 (d, J = 6.5 Hz, 1H, NH), 7.99 (t, J = 5 Hz, 1H, NH), 8.39 (m, 2H, NH), 9.15 (s, 1H, OH), 12.15 (bs, 3H, COOH). MS m/z calcd for $C_{39}H_{55}N_9O_{16}$ 905; found 906.3 [M+H$^+$]. Rt = 6.9 min (10−50% of solvent B in 16 min, purity 98%).

Peptide 5 c[YYAEGLEE]-NH$_2$. Yield: 20 mg, 8.4%. ^{1}H NMR (DMSO-d_6): 0.83 (d, J = 6.5 Hz, 3H, CH$_3$), 0.87 (d, J = 6.5 Hz, 3H, CH$_3$), 1.24 (d, J = 7.5 Hz, 3H, CH$_3$), 1.50 (m, 2H), 1.61 (m, 1H), 1.72 (m, 1H), 1.81 (m, 3H), 2.02 (m, 3H), 2.22 (m, 5H), 2.58 (m, 1H), 2.82 (m, 2H), 2.98 (m, 1H), 3.53 (dd, J = 16.5 Hz, J = 5 Hz, 1H), 3.81 (dd, J = 16.5 Hz, J = 5 Hz, 1H), 4.02 (m, 1H), 4.08 (m, 3H), 4.16 (m, 1H), 4.19 (m, 1H), 4.26 (m, 1H), 6.62 (d, J = 9 Hz, 2H), 6.65 (d, J = 9 Hz, 2H), 6.92 (d, J = 9 Hz, 2H), 6.99 (d, J = 9 Hz, 2H), 7.03 (s, 1H, CONH$_2$), 7.10 (s, 1H, CONH$_2$), 7.71 (m, 2H, NH), 7.83 (m, 2H, NH), 7.94 (d, J = 6.5 Hz, 1H, NH), 8.04 (m, 3H, NH), 8.39 (m, 2H, NH), 9.15 (bs, 2H, OH), 12.08 (bs, 2H, COOH). MS m/z calcd for $C_{44}H_{59}N_9O_{15}$ 953; found 954.4 [M+H$^+$]. Rt = 13.7 min (10−66% of solvent B in 21 min, purity 98%).

Peptide 6 c[YYDAGLEE]-NH$_2$. Yield: 20 mg, 8.5%. ^{1}H NMR (DMSO-d_6): 0.84 (d, J = 6.5 Hz, 3H, CH$_3$), 0.88 (d, J = 6.5 Hz, 3H, CH$_3$), 1.20 (d, J = 7.5 Hz, 3H, CH$_3$), 1.51 (m, 2H), 1.65 (m, 2H), 1.72 (m, 1H), 1.82 (m, 2H), 2.07 (m, 2H), 2.27 (m, 2H), 2.58 (m, 2H), 2.82 (m, 3H), 2.92 (m, 1H), 3.56 (dd, J = 16.5 Hz, J = 5.7 Hz, 1H), 3.76 (dd, J = 16.5 Hz, J = 5.7 Hz, 1H), 4.08 (m, 3H), 4.18 (m, 2H), 4.30 (m, 2H), 6.63 (d, J = 8.5 Hz, 2H), 6.65 (d, J = 8.5 Hz, 2H), 6.96 (d, J = 8.5 Hz, 2H), 6.99 (d, J = 8.5 Hz, 2H), 7.03 (s, 1H, CONH$_2$), 7.05 (s, 1H, CONH$_2$), 7.55 (d, J = 8.4 Hz, 1H, NH), 7.66 (d, J = 8.4 Hz, 1H, NH), 7.73 (d, J = 7.8 Hz, 1H, NH), 7.79 (d, J = 7.2 Hz, 1H, NH), 7.82 (d, J = 7.2 Hz, 1H, NH), 8.08 (t, J = 5.8 Hz, 1H, NH), 8.25 (t, J = 4.5 Hz, 1H, NH), 8.32 (t, J = 7.1 Hz, 1H, NH), 9.15 (bs, 2H, OH), 12.24 (bs, 2H, COOH). MS m/z calcd for $C_{43}H_{57}N_9O_{15}$ 939; found 940.5 [M+H$^+$]. Rt = 12.7 min (20−50% of solvent B in 12.8 min, purity 95%).

Peptide 7 c[YYDEALEE]-NH$_2$. Yield: 18 mg, 7%. ^{1}H NMR (DMSO-d_6): 0.84 (d, J = 6.5 Hz, 3H, CH$_3$), 0.88 (d, J = 6.5 Hz, 3H, CH$_3$), 1.25 (d, J = 7.0 Hz, 3H, CH$_3$), 1.46 (m, 1H), 1.54 (m, 1H), 1.64 (m, 2H), 1.82 (m, 4H), 2.05 (m, 3H), 2.23 (m, 4H), 2.60 (m, 2H), 2.79 (m, 3H), 2.95 (m, 1H), 4.08 (m, 3H), 4.14 (m, 1H), 4.19 (m, 1H), 4.23 (m, 2H), 4.32 (m, 1H), 6.62 (d, J = 8.5 Hz, 2H), 6.65 (d, J = 8.5 Hz, 2H), 6.96 (m, 4H), 7.03 (s, 2H, CONH$_2$), 7.57 (d, J = 7.7 Hz, 1H, NH), 7.63 (d, J = 7.6 Hz, 1H, NH), 7.65 (d, J = 9 Hz, 1H, NH), 7.73 (d, J = 8.3 Hz, 1H, NH), 7.79 (d, J = 5.3 Hz, 1H, NH), 7.87 (d, J = 6.3 Hz, 1H, NH), 8.21 (t, J = 4.4 Hz, 1H, NH), 8.39 (t, J = 6.7 Hz, 1H, NH), 9.12 (s, 1H, OH), 9.15 (s, 1H, OH), 12.08 (bs, 2H, COOH), 12.29 (bs, 1H, COOH). MS m/z calcd for $C_{46}H_{61}N_9O_{17}Na$ 1011; found 1012.3 [M+H$^+$]. Rt = 12.7 min (10−90% of solvent B in 16 min, purity 96%).

Peptide 8 c[YYDEGAEE]-NH$_2$. Yield: 13 mg, 5%. ^{1}H NMR (DMSO-d_6): 1.25 (d, J = 7.3 Hz, 3H, CH$_3$), 1.74 (m, 1H), 1.82 (m, 2H), 1.90 (m, 1H), 2.05 (m, 2H), 2.25 (m, 6H), 2.54 (m, 1H), 2.60 (m, 1H), 2.81 (m, 3H), 2.95 (m, 1H), 3.58 (dd, J = 16.3 Hz, J = 5 Hz, 1H), 3.77 (dd, J = 16.3 Hz, J = 5 Hz, 1H), 4.02 (m, 1H), 4.14 (m, 4H), 4.27 (m, 2H), 6.62 (d, J = 8.2 Hz, 2H), 6.66 (d, J = 8.2 Hz, 2H), 6.93 (bs, 1H, CONH$_2$), 6.96 (d, J = 8.2 Hz, 2H), 6.99 (d, J = 8.5 Hz, 2H), 7.08 (s, 1H, CONH$_2$), 7.63 (d, J = 8.8 Hz, 1H, NH), 7.69 (d, J = 7.6 Hz, 1H, NH), 7.78 (d, J = 6.8 Hz, 1H, NH), 7.88 (d, J = 6.8 Hz, 1H, NH), 8.01 (t, J = 4.9 Hz, 1H, NH), 8.06 (d, J = 5.9 Hz, 1H, NH), 8.2 (d, J = 4.5 Hz, 1H, NH), 8.27 (d, J = 5.5 Hz, 1H, NH), 9.14 (s, 1H, OH), 9.16 (s, 1H, OH), 12.12 (bs, 2H, COOH), 12.31 (bs, 1H, COOH). MS m/z calcd for $C_{42}H_{53}N_9O_{17}$ 955; found 956.1 [M+H$^+$]. Rt = 5.2 min (20−50% of solvent B in 16 min, purity 95%).

Peptide 9 c[YYDEGLAE]-NH$_2$. Yield: 20 mg, 8.5%. ^{1}H NMR (DMSO-d_6): 0.83 (d, J = 6.0 Hz, 3H, CH$_3$), 0.88 (d, J = 6.0 Hz, 3H, CH$_3$), 1.28 (d, J = 7.3 Hz, 3H, CH$_3$), 1.51 (m, 2H), 1.65 (m, 1H), 1.72 (m, 1H), 1.82 (m, 1H), 1.90 (m, 1H), 2.05 (m, 2H), 2.19 (m, 2H), 2.32 (m, 1H), 2.54 (m, 1H), 2.63 (m, 1H), 2.81 (m, 3H), 2.90 (m, 1H), 3.59 (dd, J = 16.7 Hz, J = 5.7 Hz, 1H), 3.79 (dd, J = 16.3 Hz, J = 5.7 Hz, 1H), 4.02 (m, 1H), 4.09 (m, 2H), 4.13 (m, 2H), 4.24 (m, 1H), 4.33 (m, 1H), 6.63 (d, J = 8.2 Hz, 2H), 6.66 (d, J = 8.6 Hz, 2H), 6.93 (bs, 1H, CONH$_2$), 6.97 (d, J = 8.6 Hz, 2H), 7.00 (d, J = 8.6 Hz, 2H), 7.01 (s, 1H, CONH$_2$), 7.52 (d, J = 7.8 Hz, 1H, NH), 7.62 (d, J = 7.6 Hz, 1H, NH), 7.79 (d, J = 7.6 Hz, 1H, NH), 7.85 (d, J = 6.3 Hz, 1H, NH), 7.93 (m, 2H, NH), 8.26 (d, J = 4.6 Hz, 1H, NH), 8.39 (d, J = 6.6 Hz, 1H, NH), 9.14 (s, 1H, OH), 9.17 (s, 1H, OH), 12.15 (bs, 1H, COOH), 12.35 (bs, 1H, COOH). MS m/z calcd for $C_{43}H_{57}N_9O_{15}$ 939; found 940.4 [M+H$^+$]. Rt = 12.6 min (10−90% of solvent B in 30 min, purity 95%).

Peptide 10 c[YYKEGLEE]-NH$_2$. Yield: 22 mg 8.8%. ^{1}H NMR (DMSO-d_6): 0.83 (d, J = 6.5 Hz, 3H, CH$_3$), 0.87 (d, J = 6.5 Hz, 3H, CH$_3$), 1.23 (m, 2H), 1.50 (m, 4H), 1.61 (m, 2H), 1.72 (m, 2H), 1.80 (m, 3H), 1.97 (m, 2H), 2.12 (m, 2H), 2.26 (m, 4H), 2.57 (m, 1H), 2.75 (m, 2H), 2.80 (m, 2H), 2.98 (m, 1H), 3.51 (dd, J = 16 Hz, J = 6 Hz, 1H), 3.84 (dd, J = 8.5 Hz, J = 5 Hz, 1H), 4.07 (m, 2H), 4.17 (m, 5H), 6.60 (d, J = 8.3 Hz, 2H), 6.67 (d, J = 8.3 Hz, 2H), 6.88 (d, J = 8.3 Hz, 2H), 7.01 (d, J = 8.3 Hz, 2H), 7.03 (s, 1H, CONH$_2$), 7.20 (s, 1H, CONH$_2$), 7.60 (bs, 3H, NH) 7.83 (d, J = 8.1 Hz, 1H, NH), 7.89 (m, 4H, NH), 7.97 (d, J = 6.2 Hz, 1H, NH), 8.10 (d, J = 6.8 Hz, 1H, NH), 8.15 (t, J = 5.5 Hz, 1H, NH), 9.15 (bs, 1H, OH), 9.18 (bs, 1H, OH), 12.08 (bs, 2H, COOH). MS m/z calcd for $C_{47}H_{66}N_{10}O_{15}$ 1010; found 1011.3 [M+H$^+$]. Rt = 11.9 min (10−90% of solvent B in 30 min, purity 100%).

Peptide 11 c[YYFEGLEE]-NH$_2$. Yield: 9 mg, 3%. ^{1}H NMR (DMSO-d_6): 0.84 (d, J = 6.5 Hz, 3H, CH$_3$), 0.88 (d, J = 6.5 Hz, 3H, CH$_3$), 1.51 (m, 1H), 1.65 (m, 1H), 1.71 (m, 1H), 1.85 (m, 3H), 2.02 (m, 3H), 2.15 (m, 3H), 2.26 (m, 3H), 2.54 (m, 1H), 2.79 (m, 3H), 2.99 (m, 1H), 3.09 (m, 1H), 3.56 (dd, J = 16.5 Hz, J = 5 Hz, 1H), 3.81 (dd, J = 16.5 Hz, J = 5 Hz, 1H), 4.07 (m, 4H), 4.17 (m, 1H), 4.24 (m, 2H), 6.62 (d, J = 9 Hz, 4H), 6.89 (d, J = 9 Hz, 2H), 7.02 (bs, 1H, CONH$_2$), 7.06 (bs, 1H, CONH$_2$), 7.20 (m, 3H), 7.26 (m, 2H), 7.62 (d, J = 8 Hz, 1H, NH), 7.73 (d, J = 8.7 Hz, 1H, NH), 7.76 (d, J = 7.1 Hz, 1H, NH), 7.94 (d, J = 7 Hz, 1H, NH), 7.97 (d, J = 7 Hz, 1H, NH), 8.06 (d, J = 4.3 Hz, 1H, NH), 8.09 (d, J = 5 Hz, 1H, NH), 9.14 (s, 1H, OH), 9.15 (s, 1H, OH), 12.07 (bs, 2H, COOH). MS m/z calcd for $C_{50}H_{63}N_9O_{15}$ 1029; found 1030.2 [M+H$^+$]. Rt = 16.2 min (10−90% of solvent B in 30 min, purity 97%).

Peptide 12 c[YYDEKLEE]-NH$_2$. Yield: 20 mg, 8%. ^{1}H NMR (DMSO-d_6): 0.84 (d, J = 6.5 Hz, 3H, CH$_3$), 0.88 (d, J = 6.5 Hz, 3H, CH$_3$), 1.33 (m, 2H), 1.51 (m, 5H), 1.63 (m, 2H), 1.72 (m, 1H), 1.81 (m, 2H), 1.90 (m, 1H), 2.03 (m, 3H), 2.13 (m, 1H), 2.27 (m, 4H), 2.60 (m, 2H), 2.79 (m, 5H), 2.95 (m, 1H), 3.99 (m, 2H),

4.06 (m, 1H), 4.12 (m, 1H), 4.18 (m, 1H), 4.28 (m, 2H), 4.40 (m, 1H), 6.62 (d, J = 8.5 Hz, 2H), 6.65 (d, J = 8.5 Hz, 2H), 6.96 (d, J = 8.5 Hz, 2H), 6.97 (d, J = 8.5 Hz, 2H), 7.03 (s, 2H, $CONH_2$), 7.44 (d, J = 7.1 Hz, 1H, NH), 7.53 (d, J = 8.1 Hz, 1H, NH), 7.60 (t, J = 4.7 Hz, 3H, NH), 7.67 (d, J = 7.9 Hz, 1H, NH), 7.70 (m, 2H, NH), 7.96 (m, 1H, NH), 8.26 (d, J = 6.8 Hz, 1H, NH), 8.42 (d, J = 4.9 Hz, 1H, NH), 9.13 (s, 1H, OH), 9.19 (s, 1H, OH), 12.10 (bs, 2H, COOH), 12.35 (bs, 1H, COOH). MS m/z calcd for $C_{49}H_{69}N_{10}O_{17}$ 1068; found 1069.4 [M+H$^+$]. Rt = 12.1 min (10−90% of solvent B in 30 min, purity 100%).

Peptide 13 c[YYDEFLEE]-NH_2. Yield: 17 mg, 6.3%. ^{1}H NMR (DMSO-d_6): 0.84 (d, J = 6.5 Hz, 3H, CH_3), 0.87 (d, J = 6.5 Hz, 3H, CH_3), 1.46 (m, 1H), 1.56 (m, 2H), 1.68 (m, 1H), 1.84 (m, 4H), 1.98 (m, 1H), 2.06 (m, 1H), 2.22 (m, 5H), 2.27 (m, 4H), 2.56 (m, 1H), 2.64 (m, 2H), 2.82 (m, 4H), 2.98 (dd, J = 14.4 Hz, J = 5.2 Hz, 1H), 3.17 (dd, J = 14.4 Hz, J = 4.5 Hz, 1H), 3.98 (m, 1H), 4.04 (m, 1H), 4.10 (m, 2H), 4.20 (m, 2H), 4.28 (m, 1H), 4.39 (m, 1H), 6.63 (d, J = 8.5 Hz, 2H), 6.64 (d, J = 8.5 Hz, 2H), 6.91 (d, J = 8.5 Hz, 2H), 6.97 (d, J = 8.5 Hz, 2H), 7.07 (s, 2H, $CONH_2$), 7.18 (t, J = 6.5 Hz, 1H), 7.26 (m, 4H), 7.60 (d, J = 8.4 Hz, 1H, NH), 7.64 (bs, 1H, NH), 7.73 (bs, 1H, NH), 7.76 (d, J = 7.6 Hz, 1H, NH), 7.81 (d, J = 5.9 Hz, 1H, NH), 7.87 (bs, 1H, NH), 8.27 (d, J = 6.4 Hz, 1H, NH), 8.38 (bs, 1H, NH), 9.14 (s, 2H, OH), 12.08 (bs, 3H, COOH). MS m/z calcd for $C_{52}H_{65}N_9O_{17}Na$ 1087; found 1110.3 [M+Na$^+$]. Rt = 16.1 min (10−90% of solvent B in 30 min, purity 96%).

Peptide 14 c[(*D*Y)YDEGLEE]-NH_2. Yield: 35 mg 14%. ^{1}H NMR (DMSO-d_6): 0.85 (d, J = 6.5 Hz, 3H, CH_3), 0.90 (d, J = 6.5 Hz, 3H, CH_3), 1.55 (m, 2H), 1.67 (m, 2H), 1.85 (m, 2H), 2.01 (m, 5H), 2.17 (m, 2H), 2.25 (m, 2H), 2.57 (m, 2H), 2.67 (m, 1H), 2.69 (m, 1H), 2.78 (m, 1H), 2.85 (m, 1H), 3.52 (dd, J = 16.5 Hz, J = 5 Hz, 1H), 3.87 (dd, J = 16.5 Hz, J = 5 Hz, 1H), 4.11 (m, 3H), 4.18 (m, 2H), 4.39 (m, 1H), 4.49 (m,1H), 6.57 (d, J = 8 Hz, 2H), 6.66 (d, J = 8 Hz, 2H), 6.77 (d, J = 8 Hz, 2H), 7.07 (d, J = 8 Hz, 2H), 7.04 (s, 1H, $CONH_2$), 7.07 (s, 1H, $CONH_2$), 7.35 (d, J = 9 Hz, 1H, NH), 7.73 (m, 2H, NH), 7.81 (t, J = 9 Hz, 1H, NH), 8.04 (t, J = 9 Hz, 1H, NH), 8.20 (d, J = 9 Hz, 1H, NH), 8.30 (d, J = 9 Hz, 1H, NH), 8.47 (d, J = 9 Hz, 1H, NH), 9.10 (s, 1H, OH), 9.15 (s, 1H, OH), 12.04 (bs, 2H, COOH), 12.26 (bs, 1H, COOH). MS m/z calcd for $C_{45}H_{59}N_9O_{17}$ 997; found 1020.4 [M+Na$^+$]. Rt = 13.8 min (20−50% of solvent B in 16 min, purity 96%).

Peptide 15 c[YKDEGLEE]-NH_2. Yield: 29 mg, 12%. ^{1}H NMR (DMSO-d_6): 0.84 (d, J = 6.5 Hz, 3H, CH_3), 0.88 (d, J = 6.5 Hz, 3H, CH_3), 1.27 (m, 2H), 1.51 (m, 4H), 1.66 (m, 4H), 1.85 (m, 3H), 2.02 (m, 3H), 2.15 (m, 1H), 2.27 (m, 4H), 2.58 (m, 1H), 2.60 (m, 1H), 2.75 (m, 4H), 2.96 (m, 1H), 3.60 (dd, J = 16.5 Hz, J = 5 Hz, 1H), 3.80 (dd, J = 16.5 Hz, J = 5 Hz, 1H), 3.90 (m, 1H), 4.04 (m, 1H), 4.10 (m, 1H), 4.18 (m, 2H), 4.27 (m, 1H), 4.38 (m, 1H), 6.64 (d, J = 9 Hz, 2H), 7.02 (bs, 1H, $CONH_2$), 7.04 (d, J = 9 Hz, 2H), 7.05 (bs, 1H, $CONH_2$), 7.60 (m, 5H, NH), 7.73 (d, J = 8.7 Hz, 1H, NH), 7.80 (d, J = 7.1 Hz, 1H, NH), 7.89 (d, J = 7.1 Hz, 1H, NH), 7.99 (t, J = 5 Hz, 1H, NH), 8.34 (d, J = 4.3 Hz, 1H, NH), 8.41 (d, J = 6.9 Hz, 1H, NH), 9.17 (s, 1H, OH), 12.15 (bs, 2H, COOH), 12.31 (bs, 1H, COOH). MS m/z calcd for $C_{42}H_{62}N_{10}O_{16}$ 962; found 963.3 [M+H$^+$]. Rt = 10.3 min (10−90% of solvent B in 30 min, purity 98%).

Peptide 16 c[YYDEGLE]-NH_2. Yield: 25 mg, 12%. ^{1}H NMR (DMSO-d_6): 0.83 (d, J = 6.2 Hz, 3H, CH_3), 0.89 (d, J = 6.2 Hz, 3H, CH_3), 1.57 (m, 3H), 1.79 (m, 2H), 1.90 (m, 1H), 1.96 (m, 1H), 2.07 (m, 1H), 2.25 (m, 1H), 2.34 (m, 2H), 2.59 (m, 3H), 2.78 (m, 1H), 2.90 (m, 1H), 3.03 (m, 1H), 3.59 (dd, J = 16.7 Hz, J = 5.3 Hz, 1H), 3.79 (dd, J = 16.7 Hz, J = 5.3 Hz, 1H), 4.01 (m, 2H), 4.09 (m, 1H), 4.18 (m, 2H), 4.30 (m, 1H), 6.60 (d, J = 8.2 Hz, 2H), 6.65 (d, J = 8.6 Hz, 2H), 6.85 (d, J = 8.6 Hz, 2H), 6.92 (d, J = 8.6 Hz, 2H), 6.93 (bs, 1H, $CONH_2$), 7.00 (s, 1H, $CONH_2$), 7.65 (d, J = 8.3 Hz, 1H, NH), 7.86 (d, J = 6.7 Hz, 1H, NH), 7.93 (m, 1H, NH), 7.99 (m, 2H, NH), 8.07 (t, J = 5.3 Hz, 1H, NH), 8.31 (d, J = 6.0 Hz, 1H, NH), 9.14 (s, 2H, OH), 12.09 (bs, 1H, COOH), 12.25 (bs, 1H, COOH). MS m/z calcd for $C_{40}H_{52}N_8O_{14}$ 868 ; found 869.4 [M+H$^+$]. Rt = 13.0 min (10−90% of solvent B in 30 min, purity 97%).

Peptide 17 c[YYDELE]-NH_2. Yield: 20 mg, 10%. ^{1}H NMR (DMSO-d_6): 0.85 (d, J = 6.4 Hz, 3H, CH_3), 0.91 (d, J = 6.4 Hz, 3H, CH_3), 1.51 (m, 2H), 1.69 (m, 2H), 1.90 (m, 1H), 2.07 (m, 3H), 2.26 (m, 1H), 2.39 (m, 2H), 2.59 (m, 1H), 2.74 (m, 4H), 2.89 (m, 1H), 3.77 (m, 1H), 4.09 (m, 2H), 4.22 (q, J = 6.3 Hz, 1H), 4.27 (q, J = 6.3 Hz, 1H), 4.45 (q, J = 6.3 Hz, 1H), 6.58 (d, J = 8.2 Hz, 2H), 6.64 (d, J = 8.2 Hz, 2H), 6.70 (d, J = 8.2 Hz, 2H), 6.94 (d, J = 8.2 Hz, 2H), 7.03 (bs, 1H, $CONH_2$), 7.08 (s, 1H, $CONH_2$), 7.64 (d, J = 8.0 Hz, 1H, NH), 7.68 (d, J = 8.0 Hz, 1H, NH), 7.95 (m, 2H, NH), 8.04 (d, J = 7.1 Hz, 1H, NH), 8.28 (d, J = 6.7 Hz, 1H, NH), 9.12 (s, 1H, OH), 9.16 (s, 1H, OH), 12.24 (bs, 2H, COOH). MS m/z calcd for $C_{38}H_{49}N_7O_{13}$ 811; found 812.1 [M+H$^+$]. Rt = 10.25 min (10−90% of solvent B in 30 min, purity 100%).

Peptide 18 c[YYELE]-NH_2. Yield: 16 mg, 9%. ^{1}H NMR (DMSO-d_6): 0.84 (d, J = 6.4 Hz, 3H, CH_3), 0.89 (d, J = 6.4 Hz, 3H, CH_3), 1.54 (m, 1H), 1.76 (m, 3H), 1.89 (m, 2H), 2.17 (m, 2H), 2.26 (m, 3H), 2.54 (m, 1H), 2.74 (m, 4H), 2.96 (m, 1H), 3.10 (m, 1H), 3.84 (m, 1H), 3.91 (m, 1H), 3.96 (m, 1H), 4.10 (m, 1H), 6.62 (d, J = 8.2 Hz, 2H), 6.65 (d, J = 8.2 Hz, 2H), 6.92 (m, 3H), 6.98 (d, J = 8.2 Hz, 2H), 7.03 (bs, 1H, $CONH_2$), 7.17 (d, 1H, NH), 7.67 (d, J = 8.0 Hz, 1H, NH), 7.79 (d, J = 8.0 Hz, 1H, NH), 7.87 (m, 2H, NH), 8.62 (d, J = 6.7 Hz, 1H, NH), 9.12 (s, 1H, OH), 9.16 (s, 1H, OH), 12.04 (bs, 1H, COOH). MS m/z calcd for $C_{34}H_{44}N_6O_{10}$ 696; found 697.2 [M+H$^+$]. Rt = 13.0 min (10−90% of solvent B in 30 min, purity 100%).

NMR Experiments and Data Processing. For chemical shift mapping (CSM) interaction studies, the sample consisted of 200 μM ^{15}N-labeled VEGFR-1D2 protein, in 90% H_2O/10% D_2O (v/v), containing 50 mM Tris and 100 mM NaCl. NMR experiments were recorded on a Varian INOVA 600 MHz spectrometer equipped with a cold-probe at 298 K. Two-dimensional ^{15}N−^{1}H HSQC NMR spectra were performed with pulse field gradient and water flip-back methods.[52] Data were acquired with 32 transients per t_1 value. Presaturation of water was employed during a recycle delay of 1.5 s. 1K complex points were acquired in t_2, with an acquisition time of 102.5 ms, while 128 complex points were acquired in t_1 with an acquisition time of 64 ms. The program NEASY, a tool of CARA software package, was utilized to analyze and assign the spectra.[53] Proton and ^{15}N assignments of the VEGFR-1_{D2} protein have been previously described by Skelton and co-workers.[44] Two-dimensional ^{15}N−^{1}H HSQC data were acquired on the VEGFR-1_{D2}/peptide complexes at the following molar ratios: 0.25:1, 0.50:1, 0.75:1, 1:1, and 2:1. To determine the per residue chemical shift perturbation upon binding and account for differences in spectral widths between ^{15}N and ^{1}H resonances, weighted average chemical shift differences, $\Delta\delta HN_{av}$, were calculated for the amide ^{15}N and ^{1}H resonances, using the following equation proposed by Garrett et al.: $\Delta\delta HN_{av(ppm)} = [(0.17\Delta N)^2 + (\Delta H)^2]^{1/2}$ where $\Delta\delta N$ and $\Delta\delta H$ are the differences between free and bound chemical shifts.[54] The weighted average chemical shift differences were mapped to the VEGFR-1_{D2} NMR structure (pdb code: 1QSV)[44] using MOLMOL graphics program.[55]

Biological Reagents. Human recombinant vascular growth factor ($VEGF_{165}$) was from Invitrogen (Carlsbad, CA, USA), Matrigel from BD Biosciences (Bedford, MA, USA), antiphospho human VEGFR-1 polyclonal antibody from Millipore (Billerica, MA, USA), antiphospho human VEGFR-2 monoclonal antibody and antiphospho human ERK1/2 monoclonal antibody from Cell Signaling (Beverly, MA, USA), antihuman α-tubulin monoclonal antibody from Euromedex (Souffelweyersheim, France), antirabbit and mouse IgG-horseradish peroxidase conjugates antibody, AMDEX streptavidin horseradish peroxydase from Amersham Biosciences (Buckinghamshire, UK), antihuman VEGFR-1 antibody, antihuman VEGFR-2 antibody, biotinylated human VEGF, recombinant human VEGFR-1_{ECD}/Fc chimera, recombinant human VEGFR-$1_{D1\text{-}D3}$ domains/Fc chimera and recombinant human VEGFR-2_{ECD}/Fc chimera from RD System (Abingdon, UK).

Chemiluminescent Competition Assays on Human Recombinant VEGFR-1. The assay was performed as previously described.[32] Briefly, a fixed amount of biotinylated human $VEGF_{165}$ (131 pM) was incubated with the tested ligands on a 96-well microplate coated by either human VEGFR-1_{ECD}/Fc chimera (20 ng/well) or VEGFR-$1_{D1\text{-}D3}$/Fc chimera (15 ng/well). The remaining biotinylated $VEGF_{165}$ after washes was detected by chemiluminescence using HRP-conjugated streptavidin.

Cell Line and Culture. HUVEC and the endothelial cell basal medium (EBM-2) supplemented with hEGF, hydrocortisone, gentamicin, amphotericin-B, VEGF, hFGF-B, R^3- IGF-1, ascorbic acid, heparin (EGM-2 bulletkit), and fetal bovin serum (FBS) were purchased from Lonza (Verviers, Belgium). HUVEC were cultured in EGM-2 at 37 °C in a humidified atmosphere containing 5% CO_2, and the medium was changed every two days. HUVEC were used from the second to the fifth passages for the experiments.

Western Blot Analysis. Experiments were performed as previously described[23] with some modifications. Confluent HUVEC in 6-well plates were starved overnight in EBM-2 without supplements. HUVEC were pretreated for 1 h by compounds and then stimulated by $VEGF_{165}$ at the indicated concentration. HUVEC were then lysed by a NP40 plus Bridj 96 lysis buffer (NP40 1%, Bridj 96 1%, Glycerol 10%, EDTA 1 mM, Tris HCl pH 7,5, Na_3VO_4 1 mM, NaF 1 mM, PMSF 1 mM, and one protease inhibitors cocktail tablet; Complete, Roche, Meylan, France). Equal amounts of proteins were loaded on SDS−polyacrylamide gel and then transferred onto nitrocellulose membranes (Bio-Rad Laboratories, Marne la Coquette, France). Membranes were incubated with the indicated antibodies at a 1:1000 dilution except for antitubulin antibody at a 1:20 000 dilution in Tris-HCl buffered saline (TBS) containing 0.1% Tween 20 (TBST) and 4% FBS overnight at 4 °C. After washes, the membranes were incubated with antirabbit IgG-horseradish peroxidase at a 1:6000 dilution and then revealed by enhanced chemiluminescence using a CCD camera (Fisher Bioblock Scientific, Illkirch, France). Densitometry analysis was performed via Chemicapt 3000 software (Fisher Bioblock Scientific, Illkirch, France). Results are expressed considering untreated wells (without VEGF) as 100% and normalized by the tubulin control.

Pull-down Assay. One milligram of the peptides was coupled to 1 mL of CNBr-activated Sepharose 4B (Pharmacia, Piscataway, NJ) as previously described.[51] Coupling yield was measured by OD at 562 nm, using BCA kit assay (Interchim, Montluçon, France) and was found at about 70%. Thirty microliters of beads (25 nmol of peptide **12**) were then incubated overnight at 4 °C in a total volume of 700 μL of TBS (Tris-base 0.025 M pH = 7.4 buffer containing 0.14 M NaCl, 0.003 M KCl) with 3 pmol of either VEGFR-1_{ECD}/Fc chimeras or VEGFR-2_{ECD}/Fc chimeras. Beads were washed 3 times with TBS containing 0.05% Tween 20. Precipitated proteins were eluted by boiling SDS sample buffer for 5 min. After SDS-PAGE separation and transfer, VEGFRs were detected by an anti-VEGFR-1 or anti-VEGFR-2 antibody and revealed by enhanced chemiluminescence using a CCD camera (Fisher Bioblock Scientific, Illkirch, France), and densitometry analysis was performed via *Chemicapt 3000* software (Fisher Bioblock Scientific, Illkirch, France).

Statistical Analysis. Each experiment was performed in triplicate. The data are expressed as mean ± SD. The statistically significant differences between the groups were determined via a two-way ANOVA followed by the Student's *t* test using Graphpad *Prism 4*. $p < 0.05$ was considered significant.

Acknowledgment. Financial support for this work was provided by the Ligue Nationale Contre le Cancer and the University Paris Descartes 'Bonus-Qualité-Recherche' grant.

Supporting Information Available: ^{1}H NMR spectra and analytical data for the peptides **1**−**18**. This material is available free of charge via the Internet at http://pubs.acs.org.

References

(1) Ferrara, N.; Kerbel, R. S. Angiogenesis as a therapeutic target. *Nature* **2005**, *438*, 967–974.
(2) Carmeliet, P.; Jain, R. K. Angiogenesis in cancer and other diseases. *Nature* **2000**, *407*, 249–257.
(3) Takahashi, H.; Shibuya, M. The vascular endothelial growth factor (VEGF)/VEGF receptor system and its role under physiological and pathological conditions. *Clin. Sci.* (*London*) **2005**, *109*, 227–241.
(4) Carmeliet, P. Angiogenesis in life, disease and medicine. *Nature* **2005**, *438*, 932–936.
(5) Folkman, J. Tumor angiogenesis: therapeutic implications. *N. Engl. J. Med.* **1971**, *285*, 1182–1186.
(6) Jain, R. K. Normalization of tumor vasculature: an emerging concept in antiangiogenic therapy. *Science* **2005**, *307*, 58–62.
(7) Shinkaruk, S.; Bayle, M.; Lain, G.; Deleris, G. Vascular endothelial cell growth factor (VEGF), an emerging target for cancer chemotherapy. *Curr. Med. Chem. Anticancer Agents* **2003**, *3*, 95–117.
(8) Ellis, L. M.; Hicklin, D. J. VEGF-targeted therapy: mechanisms of anti-tumour activity. *Nat. Rev. Cancer* **2008**, *8*, 579–591.
(9) Ferrara, N.; Gerber, H. P.; LeCouter, J. The biology of VEGF and its receptors. *Nat. Med.* **2003**, *9*, 669–676.
(10) Roskoski, R., Jr. Vascular endothelial growth factor (VEGF) signaling in tumor progression. *Crit. Rev. Oncol. Hematol.* **2007**.
(11) De Paepe, B. Anti-angiogenic agents and cancer: current insights and future perspectives. *Recent Pat. Anticancer Drug Discovery* **2009**, *4*, 180–185.
(12) Ferrara, N.; Hillan, K. J.; Novotny, W. Bevacizumab (Avastin), a humanized anti-VEGF monoclonal antibody for cancer therapy. *Biochem. Biophys. Res. Commun.* **2005**, *333*, 328–335.
(13) Ferrara, N.; Mass, R. D.; Campa, C.; Kim, R. Targeting VEGF-A to treat cancer and age-related macular degeneration. *Annu. Rev. Med.* **2007**, *58*, 491–504.
(14) Lau, S. C.; Rosa, D. D.; Jayson, G. Technology evaluation: VEGF Trap (cancer), Regeneron/sanofi-aventis. *Curr. Opin. Mol. Ther.* **2005**, *7*, 493–501.
(15) Gerber, D. Targeted therapies: a new generation of cancer treatments. *Am. Acad. Family Physicians* **2008**, *77*, 311–319.
(16) Wilhelm, S. M.; Adnane, L.; Newell, P.; Villanueva, A.; Llovet, J. M.; Lynch, M. Preclinical overview of sorafenib, a multikinase inhibitor that targets both Raf and VEGF and PDGF receptor tyrosine kinase signaling. *Mol. Cancer Ther.* **2008**, *7*, 3129–3140.
(17) Faivre, S.; Demetri, G.; Sargent, W.; Raymond, E. Molecular basis for sunitinib efficacy and future clinical development. *Nat. Rev. Drug Discovery* **2007**, *6*, 734–745.
(18) Posey, J. A.; Ng, T. C.; Yang, B.; Khazaeli, M. B.; Carpenter, M. D.; Fox, F.; Needle, M.; Waksal, H.; LoBuglio, A. F. A phase I study of anti-kinase insert domain-containing receptor antibody, IMC-1C11, in patients with liver metastases from colorectal carcinoma. *Clin. Cancer Res.* **2003**, *9*, 1323–1332.
(19) DeLano, W. L. Unraveling hot spots in binding interfaces: progress and challenges. *Curr. Opin. Struct. Biol.* **2002**, *12*, 14–20.
(20) Veslovsky, A. V.; Archakov, A. I. Inhibitors of protein-protein interaction as potential drugs. *Curr. Comput.-Aided Drug Des.* **2007**, *3*, 51–58.
(21) D'Andrea, L. D.; Del Gatto, A.; De Rosa, L.; Romanelli, A.; Pedone, C. Peptides targeting angiogenesis related growth factor receptors. *Curr. Pharm. Des.* **2009**, *15*, 2414–2429.
(22) Goncalves, V.; Gautier, B.; Garbay, C.; Vidal, M.; Inguimbert, N. Structure-based design of a bicyclic peptide antagonist of the vascular endothelial growth factor receptors. *J. Pept. Sci.* **2007**.
(23) Goncalves, V.; Gautier, B.; Coric, P.; Bouaziz, S.; Lenoir, C.; Garbay, C.; Vidal, M.; Inguimbert, N. Rational design, structure, and biological evaluation of cyclic peptides mimicking the vascular endothelial growth factor. *J. Med. Chem.* **2007**, *50*, 5135–5146.
(24) Goncalves, V.; Gautier, B.; Regazzetti, A.; Coric, P.; Bouaziz, S.; Garbay, C.; Vidal, M.; Inguimbert, N. On-resin cyclization of peptide ligands of the vascular endothelial growth factor receptor 1 by copper(I)-catalyzed 1,3-dipolar azide-alkyne cycloaddition. *Bioorg. Med. Chem. Lett.* **2007**, *17*, 5590–5594.
(25) Wiesmann, C.; Fuh, G.; Christinger, H. W.; Eigenbrot, C.; Wells, J. A.; de Vos, A. M. Crystal structure at 1.7 A resolution of VEGF in complex with domain 2 of the Flt-1 receptor. *Cell* **1997**, *91*, 695–704.

(26) Christinger, H. W.; Fuh, G.; de Vos, A. M.; Wiesmann, C. The crystal structure of placental growth factor in complex with domain 2 of vascular endothelial growth factor receptor-1. *J. Biol. Chem.* **2004**, *279*, 10382–10388.
(27) Keyt, B. A.; Nguyen, H. V.; Berleau, L. T.; Duarte, C. M.; Park, J.; Chen, H.; Ferrara, N. Identification of vascular endothelial growth factor determinants for binding KDR and FLT-1 receptors. Generation of receptor-selective VEGF variants by site-directed mutagenesis. *J. Biol. Chem.* **1996**, *271*, 5638–5646.
(28) Muller, Y. A.; Li, B.; Christinger, H. W.; Wells, J. A.; Cunningham, B. C.; de Vos, A. M. Vascular endothelial growth factor: crystal structure and functional mapping of the kinase domain receptor binding site. *Proc. Natl. Acad. Sci. U.S.A.* **1997**, *94*, 7192–7197.
(29) Li, B.; Fuh, G.; Meng, G.; Xin, X.; Gerritsen, M. E.; Cunningham, B.; de Vos, A. M. Receptor-selective variants of human vascular endothelial growth factor. Generation and characterization. *J. Biol. Chem.* **2000**, *275*, 29823–29828.
(30) Errico, M.; Riccioni, T.; Iyer, S.; Pisano, C.; Acharya, K. R.; Persico, M. G.; De Falco, S. Identification of placenta growth factor determinants for binding and activation of Flt-1 receptor. *J. Biol. Chem.* **2004**, *279*, 43929–43939.
(31) Goncalves, V. G., B.; Lenoir, C.; Garbay, C.; Vidal, M.; Inguimbert, N. Peptides as antagonists of the VEGF receptors. *PharmaChem* **2006**, 15–19.
(32) Goncalves, V.; Gautier, B.; Garbay, C.; Vidal, M.; Inguimbert, N. Development of a chemiluminescent screening assay for detection of vascular endothelial growth factor receptor 1 ligands. *Anal. Biochem.* **2007**, *366*, 108–110.
(33) Gautier, B.; Goncalves, V.; Huguenot, F.; Garbay, C.; Vidal, M.; Inguimbert, N. unpublished results.
(34) Olsson, A. K.; Dimberg, A.; Kreuger, J.; Claesson-Welsh, L. VEGF receptor signalling - in control of vascular function. *Nat. Rev. Mol. Cell Biol.* **2006**, *7*, 359–371.
(35) Chang, C. D.; Meienhofer, J. Solid-phase peptide-synthesis using mild base cleavage of nalpha-fluorenylmethyloxycarbonylamino acids, exemplified by a synthesis of dihydrosomatostatin. *Int. J. Pept. Protein Res.* **1978**, *11*, 246–249.
(36) Kates, S. A.; Sole, N. A.; Johnson, C. R.; Hudson, D.; Barany, G.; Albericio, F. A. A novel, convenient, three-dimensional orthogonal strategy for solid-phase synthesis of cyclic peptides. *Tetrahedron. Lett.* **1993**, *34*, 1549–1552.
(37) Johnson, T.; Liley, M. J.; Cheeseright, T. J.; Begum, F. Problems in the synthesis of cyclic peptides through use of the Dmab protecting group. *J. Chem. Soc., Perkin Trans.* **2000**, *43*, 2811–2820.
(38) Starzec, A.; Ladam, P.; Vassy, R.; Badache, S.; Bouchemal, N.; Navaza, A.; du Penhoat, C. H.; Perret, G. Y. Structure-function analysis of the antiangiogenic ATWLPPR peptide inhibiting VEGF(165) binding to neuropilin-1 and molecular dynamics simulations of the ATWLPPR/neuropilin-1 complex. *Peptides* **2007**, *28*, 2397–2402.
(39) Yongye, A. B.; Li, Y.; Giulianotti, M. A.; Yu, Y.; Houghten, R. A.; Martinez-Mayorga, K. Modeling of peptides containing D-amino acids: implications on cyclization. *J. Comput.-Aided Mol. Des.* **2009**, *23*, 677–689.
(40) Goncalves, V.; Gautier, B.; Huguenot, F.; Leproux, P.; Garbay, C.; Vidal, M.; Inguimbert, N. Total chemical synthesis of the D2 domain of human VEGF receptor 1. *J. Pept. Sci.* **2009**, *15*, 417–422.
(41) Chamorro, C.; Kruijtzer, J. A.; Farsaraki, M.; Balzarini, J.; Liskamp, R. M. A general approach for the non-stop solid phase synthesis of TAC-scaffolded loops towards protein mimics containing discontinuous epitopes. *Chem. Commun.* (*Camb.*) **2009**, 821–823.
(42) Barleon, B.; Totzke, F.; Herzog, C.; Blanke, S.; Kremmer, E.; Siemeister, G.; Marme, D.; Martiny-Baron, G. Mapping of the sites for ligand binding and receptor dimerization at the extracellular domain of the vascular endothelial growth factor receptor FLT-1. *J. Biol. Chem.* **1997**, *272*, 10382–10388.
(43) Lacal, P. M.; Morea, V.; Ruffini, F.; Orecchia, A.; Dorio, A. S.; Failla, C. M.; Soro, S.; Tentori, L.; Zambruno, G.; Graziani, G.; Tramontano, A.; D'Atri, S. Inhibition of endothelial cell migration and angiogenesis by a vascular endothelial growth factor receptor-1 derived peptide. *Eur. J. Cancer* **2008**, *44*, 1914–1921.
(44) Starovasnik, M. A.; Christinger, H. W.; Wiesmann, C.; Champe, M. A.; de Vos, A. M.; Skelton, N. J. Solution structure of the VEGF-binding domain of Flt-1: comparison of its free and bound states. *J. Mol. Biol.* **1999**, *293*, 531–544.
(45) Leppanen, V. M.; Prota, A. E.; Jeltsch, M.; Anisimov, A.; Kalkkinen, N.; Strandin, T.; Lankinen, H.; Goldman, A.; Ballmer-Hofer, K.; Alitalo, K. Structural determinants of growth factor binding and specificity by VEGF receptor 2. *Proc. Natl. Acad. Sci. U.S.A.* **2010**, *107*, 2425–2430.
(46) Millauer, B.; Wizigmann-Voos, S.; Schnurch, H.; Martinez, R.; Moller, N. P.; Risau, W.; Ullrich, A. High affinity VEGF binding and developmental expression suggest Flk-1 as a major regulator of vasculogenesis and angiogenesis. *Cell* **1993**, *72*, 835–846.
(47) Bernatchez, P. N.; Soker, S.; Sirois, M. G. Vascular endothelial growth factor effect on endothelial cell proliferation, migration, and platelet-activating factor synthesis is Flk-1-dependent. *J. Biol. Chem.* **1999**, *274*, 31047–31054.
(48) Waltenberger, J.; Claesson-Welsh, L.; Siegbahn, A.; Shibuya, M.; Heldin, C. H. Different signal transduction properties of KDR and Flt1, two receptors for vascular endothelial growth factor. *J. Biol. Chem.* **1994**, *269*, 26988–26995.
(49) Gille, H.; Kowalski, J.; Yu, L.; Chen, H.; Pisabarro, M. T.; Davis-Smyth, T.; Ferrara, N. A repressor sequence in the juxtamembrane domain of Flt-1 (VEGFR-1) constitutively inhibits vascular endothelial growth factor-dependent phosphatidylinositol 3′-kinase activation and endothelial cell migration. *Embo J.* **2000**, *19*, 4064–4073.
(50) Fuh, G.; Wu, P.; Liang, W. C.; Ultsch, M.; Lee, C. V.; Moffat, B.; Wiesmann, C. Structure-function studies of two synthetic anti-vascular endothelial growth factor Fabs and comparison with the Avastin Fab. *J. Biol. Chem.* **2006**, *281*, 6625–6631.
(51) Vidal, M.; Liu, W. Q.; Lenoir, C.; Salzmann, J.; Gresh, N.; Garbay, C. Design of peptoid analogue dimers and measure of their affinity for Grb2 SH3 domains. *Biochemistry* **2004**, *43*, 7336–7344.
(52) Hajduk, P. J.; Meadows, R. P.; Fesik, S. W. NMR-based screening in drug discovery. *Q. Rev. Biophys.* **1999**, *32*, 211–240.
(53) Keller, R. *The Computer Aided Resonance Assignment Tutorial*; CANTINA Verlag: Goldau, 2004.
(54) Garrett, D. S.; Seok, Y. J.; Peterkofsky, A.; Clore, G. M.; Gronenborn, A. M. Identification by NMR of the binding surface for the histidine-containing phosphocarrier protein HPr on the N-terminal domain of enzyme I of the Escherichia coli phosphotransferase system. *Biochemistry* **1997**, *36*, 4393–4398.
(55) Koradi, R.; Billeter, M.; Wuthrich, K. MOLMOL: a program for display and analysis of macromolecular structures. *J. Mol. Graph.* **1996**, *14* (51−55), 29–32.